adhesives

MDPI

Review

Measuring the Rheological, Textural, Geotechnical and Viscoelastic Behaviour of Dewatered Sludge: Including Adhesiveness and Cohesiveness

Sergio Luis Parra-Angarita [1,*], Juan Federico Herrera-Ruiz [2], Guillermo H. Gaviria [3] and Angélique Léonard [1,*]

[1] Chemical Engineering Research Unit, PEPs, University of Liège, Quartier Agora, Allée du 6 Août 11, 4000 Liège, Belgium
[2] Grupo de Investigación en Aplicación de Nuevas Tecnologías (GIANT), Departamento de Ingeniería Química, Facultad de Ingeniería y Arquitectura, Universidad Nacional de Colombia, Sede Manizales, Campus La Nubia, km 9 vía al Aeropuerto la Nubia, Manizales 170001, Caldas, Colombia; jufherreraru@unal.edu.co
[3] Grupo de Investigación en Procesos Reactivos Intensificados y Materiales Avanzados-PRISMA, Departamento de Ingeniería Química, Facultad de Ingeniería y Arquitectura, Universidad Nacional de Colombia, Sede Manizales, Campus La Nubia, km 9 vía al Aeropuerto la Nubia, Manizales 170001, Caldas, Colombia; ghgavirial@unal.edu.co
* Correspondence: slparra@uliege.be (S.L.P.-A.); a.leonard@uliege.be (A.L.)

Abstract

Mechanical properties such as viscoelastic, rheological, and textural properties, particularly adhesiveness and cohesiveness, play a significant role in the optimization of handling, processing and drying of dewatered sludge. However, there is no currently standardized methodology for quantifying these properties, leading researchers to adopt various techniques based on economic feasibility, equipment availability, and research objectives. This review systematically compiles and analyzes the most relevant experimental methodologies for evaluating the mechanical properties of dewatered sewage sludge (DSS). This work presents a general overview of the composition and structure of DSS, followed by a comprehensive bibliometric analysis that revealed literature gaps (particularly in adhesiveness evaluation) and identified regulatory frameworks that incremented interest in researching DSS' properties in the broader push for sustainability. Consequently, a discussion of the experimental set-ups, data treatment and visualization, advantages and disadvantages, and mathematical models with their physical significance is presented for the different techniques identified. The methods analyzed include oscillatory rheology, penetrometry (cylinder and cone), uniaxial compression tests (TPA), shear testing (e.g., Jenike shear test, Atterberg limit test, direct box shear test, triaxial shear test, unconfined shear test, and vane shear test), tomography and slump tests. By comparing these techniques, this study provides insights into the most appropriate approaches for sludge characterization, emphasizing the need for a unified framework to standardize the evaluation of viscoelastic and textural properties in DSS.

Keywords: sewage sludge; rheology; adhesiveness; cohesiveness; texture; viscoelasticity; bibliometrics analysis

Check for updates

Academic Editor: Vasileios Koutsos

Received: 9 April 2026
Revised: 7 July 2026
Accepted: 23 July 2026
Published: 4 August 2026

Copyright: © 2026 by the authors. Licensee MDPI, Basel, Switzerland. This article is an open access article distributed under the terms and conditions of the Creative Commons Attribution (CC BY) license.

1. Introduction

Sewage sludge (SS) constitutes the primary by-product generated at wastewater treatment plants (WWTPs), with global production estimated at 45–50 million tonnes of dry solids per year. Outside Europe, this generation continues to grow annually due to rapid

industrialization, urbanization, the expansion of sewer networks, and stricter treatment standards [1–4]. This upward trend poses a significant challenge for municipal and industrial sectors in terms of management and final disposal, exacerbated by increasingly stringent environmental regulations that limit emissions and demand higher quality of treated residues, thereby driving the adoption of more efficient and sustainable handling strategies. Among major economies, the European Union generates around 11 million tonnes [5], while the United States produces 12.55 million tonnes [6], China 15.75 million tonnes [7], Japan 2.35 million tonnes [8], and India 3.96 million tonnes of SS as dry solids (DSs) annually [9].

Traditional SS management strategies focus on reducing water content to minimize volume, stabilize organic matter, and prepare SS for disposal or valorization. Common operations include thickening, mechanical dewatering, stabilization (e.g., anaerobic digestion, liming), and thermal drying [10]. SS management may account for 20–65% of total WWTP operating costs, with thermal drying alone representing 50–70% of sludge line energy consumption [11,12]. Mechanical dewatering typically requires 0.12–0.26 kWh/kg_{DS}, while thermal drying demands 3.8 kWh/kg_{DS}, confirming drying as the most energy-intensive operation in SS treatment lines [13].

As SS progresses through the treatment line, it undergoes a marked transition from a dilute Newtonian liquid (0.5–1% of dry solids (DSs)) to a highly viscous non-Newtonian suspension (1–10% DSs after thickening) [14,15], a pasty soft solid after mechanical dewatering (20–45% DSs) [16–20] known as dewatered sewage sludge (DSS), and finally a granular dry solid (>90–95% DSs) after thermal drying [21–23]. However, it is precisely at the DSS stage (20–45% DSs) where rheological and textural properties become most critical for process efficiency [24,25].

The understanding and quantification of the rheological, textural, and viscoelastic characteristics of SS and DSS throughout its treatment line is critical for optimizing management processes [20,26,27]. While standardized protocols exist in the literature for measuring these properties in liquid SS [14,28–30], current knowledge on the mechanical, textural, and viscoelastic characterization of highly DSS (20–45% TS) remains fragmented. Most studies focus on limited property sets, test conditions, or sludge types, lacking a consolidated framework that systematically compares experimental methods for capturing adhesiveness and cohesiveness, their dependence on moisture content, composition, and conditioning, and their quantitative relationships to drying performance and full-scale operational constraints [17,18,20–24,31–39].

This review aims to provide a comprehensive overview of the state-of-the-art techniques available, serving as a valuable resource for scientists, engineers, and researchers. By offering a detailed comparison of these methods, this article seeks to lay the groundwork for future standardization efforts, ultimately leading to more consistent and comparable results in sludge characterization. Recent reviews have mainly focused on the processing of sludges in wastewater treatment processes [40]. Other reviews treating the rheology of sludges mainly focus on modelling approaches, overlooking the measurement of several properties [14,41]. These reviews are almost one decade old, and are focused on liquid sewage sludge, so this work aims to update and present current advances.

Despite the abundance of experimental studies, no recent work has systematically compared these methods specifically for highly DSS (20–45% TS), where rheological behaviour transitions from a Newtonian fluid to soft solid. Moreover, as highlighted by the bibliometric analysis conducted in this study (Section 6), the field has reached a maturation phase following rapid expansion between 2005 and 2022, indicating the need for a consolidation review that bridges rheological, textural, and geotechnical approaches. Addi-

tionally, adhesiveness, despite its critical role in drying operations, has been systematically underrepresented in the literature (Section 9).

The following paper is structured as follows:

Section 2 examines the underlying properties, composition, and microstructure of sewage sludge (SS) and the changes occurring throughout its treatment line. Section 3 presents the definitions of the studied properties, while Sections 4 and 5 focuses on micro and macro mechanisms of adhesion and cohesion and rheological, textural, and viscoelastic modelling of dewatered sewage sludge, respectively. Section 6 describes the methodology used for the Literature Review Strategy, followed by Section 7, which presents the main results of the bibliometric analysis. Section 8 provides an analysis of relevant works in the field, supporting efforts toward method standardization and the development of predictive mechanical descriptors for sludge management. Section 9 offers a comparative summary of experimental methods for sludge mechanical characterization, and finally, Section 10 gives an analysis of adhesiveness, an overlooked property in sludge mechanical characterization.

2. Composition and Structure of Sewage Sludge Through Its Treatment Line

Liquid SS constitutes a complex heterogeneous colloidal system featuring a dispersed phase of microorganisms, organic/inorganic compounds, fibres, and pollutants agglomerated into granules/clusters that further aggregate into flocs, suspended within a continuous aqueous phase containing dissolved electrolytes and salts. SS composition varies substantially depending on wastewater origin (municipal/industrial), WWTP treatment processes, geographic location, and critically total solids content (TSC) [42–44]. Table 1 presents validated typical compositions of raw SS in dry basis compiled from multiple global sources [45–49].

Water is the dominant component of SS, existing in four distinct forms that critically govern dewaterability: free water, interstitial/capillary water, surface/adsorbed water, and intracellular water. Free water remains chemically/physically unbound to flocs and exists externally; interstitial water occupies floc interiors via capillary forces within inter-particle pores; surface water binds via supramolecular forces to particle surfaces (also termed adsorbed water); and intracellular water resides within microbial cells comprising the floc matrix [50–53]. Free water is readily removed by mechanical dewatering (filtration, centrifugation), while the latter three types of collectively termed bound water demand substantial energy inputs via thermal drying, microwaves, or advanced disruption methods [1,25,54,55]. Figure 1a schematically illustrates this water distribution within SS flocs.

Microorganisms account for approximately 5–20% of the organic fraction of SS, while extracellular polymeric substances (EPSs) constitute the dominant matrix, contributing 60–90% of total organic dry mass. Polysaccharides and proteins represent the primary EPS components (70–80% combined), with proteins providing structural integrity/hydrophobic bridging and polysaccharides forming the hydrophilic gel network [56–61]. Biological aggregates (granules/clusters) arise from the accumulation of microorganisms, EPSs, multivalent cations (Ca^{2+}, Mg^{2+}, Fe^{3+}), and soluble microbial products. The widely accepted four-layer granule model stratifies structure as cell clusters (core biomass), tightly bound EPSs (TB-EPSs) (cell-adherent), loosely bound EPSs (LB-EPSs) (diffuse matrix), and soluble EPSs (S-EPSs) (free-floating exudates) [56,59,61], as illustrated in Figure 1b.

During dewatering, SS undergoes progressive structural consolidation as mechanical forces selectively remove free and interstitial water, concentrating the bound water/EPS matrix characteristic of DSS. DSS can be described as a highly concentrated, paste-like material with a heterogeneous and porous internal structure [25,51,55,62,63]. At a typical TSC of 20–45%, DSS is no longer a free-flowing slurry but a cohesive soft solid in which densely packed flocs form a continuous network, interspersed with a system of residual

micro and mesopores filled mainly with bound water [64–66]. The skeleton of this network is largely formed by compacted EPSs and cell debris, giving the material an essentially amorphous, gel-like character rather than a crystalline one [56,58,67]. After dewatering, most of the remaining moisture is present as capillary/interstitial water within small pores, surface/adsorbed water associated with hydrophilic EPSs, and water trapped within partially damaged cells, so the fraction of truly free water becomes very small [50,52,68–70]. As a result of this concentration and structural rearrangement, the relative proportion of organics (especially EPSs) increases, effective hydrophilicity remains high, and DSS exhibits strong cohesiveness and adhesiveness, which directly affects its rheological and handling behaviour [24,27,39,71]. A schematic of DSS structure is shown in Figure 1c.

During thermal drying, DSS undergoes profound textural and microstructural evolution, transforming from a cohesive paste (20–45% TSC) to a friable, granular solid (>85–95% TS) characterized by a densified, cracked matrix with significantly reduced porosity [18,21,39,63,69,72–79]. Heat-driven processes induce EPS thermal denaturation, protein aggregation (above 60–80 °C), polysaccharide caramelization/degradation, and Maillard reactions between amino acids and reducing sugars, forming a rigid, amorphous carbonaceous skeleton riddled with shrinkage cracks and vapor-induced microfractures [80–82]. Residual moisture (<2–5%) exists primarily as vicinal water tightly associated with mineral phases and humic-like residues, virtually eliminating all other kinds of water [65,73,83–86]. A schematic of dried SS structure is shown in Figure 1d.

Table 1. Raw sewage sludge min–max compositions.

Proximate Analysis					
Parameter	**Unit**	**Value**			
Volatile matter content	% of TSC	50	-	80	
Ash content		20	-	40	
Ultimate Analysis					
Parameter	**Unit**	**Value**			
C	% of TSC	25	-	58	
H		6	-	10.2	
N		1	-	9.9	
S		0.09	-	0.45	
O		10	-	20	
Metals and Heavy Metals					
Parameter	**Unit**	**Value**			**Average**
Arsenic (As)	mg/kg_{TSC}	1.1	-	230	10
Barium (Ba)		40	-	1300	50
Cadmium (Cd)		1	-	3410	10
Cobalt (Co)		11.3	-	2490	30
Copper (Cu)		84	-	17,000	800
Cromium (Cr)		10	-	99,000	500
Iron (Fe)		1000	-	15,400	17,000
Lead (Pb)		13	-	26,000	500
Manganese (Mg)		32	-	9870	260
Mercury (Hg)		0.6	-	56	6
Molybdenum (Mo)		0.1	-	214	4
Nickel (Ni)		2	-	5300	80
Selenium (Se)		1.7	-	17.2	5
Titanium (Ti)		2.6	-	329	40
Zinc (Zn)		101	-	49,000	1700

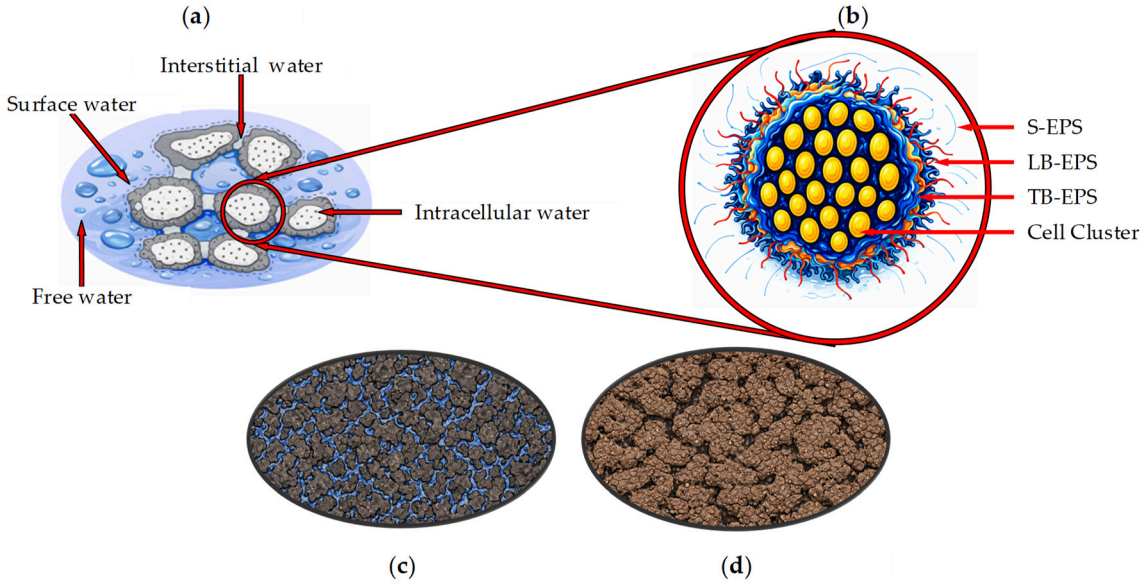


Figure 1. Structural evolution of sewage sludge during treatment adapted from [1]. (**a**) Water distribution in raw sludge (free, interstitial, adsorbed, and intracellular). (**b**) Floc structure composed of microorganisms and EPSs (TB-EPSs, LB-EPSs, S-EPSs). (**c**) Dewatered sludge structure. (**d**) Dried sludge structure.

This progression eliminates paste adhesiveness but generates friability and dustiness [80,81,87]. The resulting heterogeneous, low-porosity aggregate (no longer hydrogel-like) facilitates storage/transport but introduces challenges for rehydration and certain valorization pathways like palletization [12,88,89].

3. Rheological, Textural, Geotechnical and Viscoelastic Property Definitions

The mechanical behaviour of complex materials can be described through several complementary frameworks, including rheological, viscoelastic, textural, and geotechnical properties. These descriptors originate from different scientific disciplines, fluid mechanics, materials science, food engineering, and soil mechanics, but they all aim to quantify how a material deforms, flows, and resists mechanical stresses under different loading modes and time scales. Because many structured materials, as the DSS, exhibit both solid-like and fluid-like responses, their characterization generally requires multiple descriptors rather than a single parameter [90–93].

3.1. Geotechnical Descriptors

Geotechnical properties describe the shear strength, bearing capacity, and stability of soils and soil-like materials under various stress paths and drainage conditions. Classical parameters include liquid limit (LL), plastic limit (PL), shrinkage limit (SL), cohesion (c), internal friction angle (φ), undrained shear strength (S_u), slump (S), among others, which are typically derived from direct shear, triaxial shear, vane shear, and unconfined compression tests. These descriptors are central to evaluating slope stability, settlement, and load-bearing performance in civil and environmental engineering applications.

Geotechnical characterization has been extensively employed when sludge is disposed in landfills, used as cover material, or incorporated into soil–sludge mixtures and construction [34–36,94–98]. Shear strength parameters obtained from direct shear, triaxial, and unconfined compression tests provide critical information for assessing landfill stability, designing embankments, and determining safe stacking heights. At the same time, compar-

isons with conventional soft clays highlight the unique mechanical behaviour of sludge, strongly controlled by organic content, bound water, and EPS-mediated structure.

3.2. Rheological Descriptors

Rheology is commonly defined as the science that studies the deformation and flow behaviour of matter, encompassing both fluids and soft solids that may exhibit plastic or viscoelastic responses under applied stress [94,99]. Key rheological parameters include viscosity (η), shear stress (τ), shear rate $(\dot{\gamma})$ and yield stress (σ_o), which characterize the resistance of materials to deformation and flow under mechanical loading and are fundamental for describing transport phenomena and mechanical stability in a wide range of industrial and natural systems [94,99].

In the context of SS, rheological characterization has traditionally focused on steady and transient shear measurements to determine apparent viscosity and yield stress, particularly for thickened sludge and concentrated suspensions [15,28,30,31,100–104]. However, for DSS in the 20–45% TS range, the material progressively departs from classical Newtonian fluid behaviour and acquires soft-solid characteristics, making it necessary to pass conventional rotational rheometry to oscillatory rheometry in order to measure the viscoelastic descriptors [55,92,102,105–107].

3.3. Viscoelastic Descriptors

Viscoelastic properties arise when a material exhibits both elastic and viscous responses simultaneously. Elastic behaviour refers to the capacity of a material to store mechanical energy and recover its original shape after deformation, whereas viscous behaviour involves irreversible deformation accompanied by energy dissipation. In oscillatory mechanical tests, viscoelasticity is typically described through the storage modulus (G'), representing the elastic component of the response, and the loss modulus (G''), representing the viscous component. Changes in G' and G'' as a function of stress or strain allow the determination of the linear viscoelastic region (LVR), beyond which the elastic structure of the material is exceeded, and the flow point (FL), defined as the stress at which the material starts to flow. The ratio between these quantities, expressed as the loss tangent $\tan(\delta) = G''/G'$, indicates whether the material behaves predominantly as a solid-like or liquid-like system under dynamic deformation conditions [92,105].

For sludge systems, oscillatory rheometry has shown that at low total solids content sludge behaves mainly as a viscous fluid with $G'' > G'$, whereas at higher solids contents, particularly after mechanical dewatering, an interconnected floc network develops, leading to a predominantly gel-like response where $G' > G''$ [24,86,108]. These viscoelastic descriptors are therefore essential for interpreting structural changes along the treatment line and for supporting the analogue mechanical models presented in Section 4.

3.4. Textural Descriptors

Textural properties provide empirical descriptors of the mechanical response of soft materials subjected to deformation and are widely used in materials science and food engineering to characterize structural resistance during compression, penetration, or tensile deformation [93,99]. Typical descriptors include hardness, springiness, cohesiveness, and adhesiveness, which collectively describe the resistance to deformation, structural recovery, and detachment behaviour of a material. Unlike rheological and viscoelastic descriptors derived from constitutive relationships, textural properties are generally operational descriptors obtained from specific mechanical tests and provide practical indicators of structural organization and mechanical integrity [90–93,109].

In DSS, texture profile analysis (TPA), uniaxial compression, and penetration tests have been adapted to quantify hardness, adhesiveness, and cohesiveness, particularly in

the sticky phase where surface interactions and structural collapse strongly affect handling and drying. These empirical descriptors are especially useful for correlating mechanical behaviour with operational issues such as stickiness, caking, and loss of structural stability during storage or thermal treatment.

3.5. Cohesion and Adhesion Descriptors

Cohesion and adhesion are fundamental to the mechanical behaviour of structured materials. Cohesion refers to internal attractive forces (intermolecular interactions, capillary effects, electrostatic forces) that provide structural integrity and resistance to fracture within the material. Adhesion, in contrast, describes interfacial interactions with external surfaces, governed by van der Waals forces, hydrogen bonding, and electrostatic mechanisms. The balance between cohesive and adhesive forces determines failure modes: cohesive failure occurs within the material, whereas adhesive failure occurs at the interface [110–114]. From an experimental perspective, cohesion is typically quantified through shear, compression, or tensile tests probing internal resistance, while adhesion is measured via detachment or pull-off experiments determining interfacial separation forces.

In the specific case of DSS, the balance between cohesion and adhesion is strongly controlled by moisture content and thermal history and governs the so-called sticky phase that emerges at intermediate dry solids contents during drying. In this regime, sludge behaves as a highly cohesive, plastic–rubbery material that simultaneously exhibits strong bulk strength and intense adhesion to contact surfaces, leading to severe fouling, clogging, and loss of dryer performance [18,21,63,71–78].

4. Microscopic and Macroscopic Mechanisms of Adhesion and Cohesion in Dewatered Sewage Sludge

The macroscopic behaviour of dewatered sewage sludge is the result of several coupled microscopic mechanisms acting within the floc network and at the sludge–surface interface. At the microscopic scale, cohesion is mainly controlled by floc connectivity, EPS-mediated bridging, capillary forces, electrostatic interactions, and the distribution of bound water within the porous sludge matrix [115–117].

During dewatering, the sludge evolves from a highly hydrated flocculated suspension into a more compact paste-like matrix, as free water is removed and capillary and bound water become progressively more dominant. This consolidation increases particle packing, enhances EPS-mediated connectivity, and promotes the development of a mechanically coherent network that resists deformation but also exhibits strong stickiness in the intermediate solids range. A more connected and compact floc structure generally increases internal resistance to separation and deformation, whereas structural disruption, heterogeneous water distribution, or weak interparticle bonding reduce cohesion and promote localized failure [21,39,70,78,118,119].

Adhesion arises from interfacial interactions between the sludge surface and the contacting material and is strongly influenced by surface water, organic matter, fine particles, and the presence of mobile EPS-rich layers. In sludge systems, EPSs can enhance or weaken attachment depending on its composition and distribution, the surface properties of the contacting material, and the ionic conditions of the medium. For example, EPS interactions with hydrophilic and hydrophobic surfaces have been shown to control binding behaviour, while cationic bridging and hydrogen bonding can strengthen EPS–EPS and EPS–surface interactions. In DSS, this combination promotes the formation of a sticky interfacial film that enhances attachment to metal surfaces, probes, and processing equipment. As solids content increases during dewatering and drying, the relative balance between cohesive strength and adhesive tendency changes, producing the well-known

sticky phase in which the sludge is simultaneously deformable, surface-active, and difficult to handle [115,120–122].

At the macroscopic scale, these microscopic interactions are expressed through measurable textural and mechanical responses such as hardness, cohesiveness, adhesiveness, yield behaviour, and shear resistance. However, no single technique captures all of these features simultaneously. For this reason, texture profile analysis, penetration, compression, shear, and rheological tests should be viewed as complementary methods that probe different aspects of the same multiscale phenomenon. In the present review, adhesiveness and cohesiveness are therefore treated as central descriptors that connect sludge microstructure with operational behaviour during pumping, drying, storage, and transport [24,26,35,122,123].

5. Rheological, Textural and Viscoelastic Modelling of Dewatered Sewage Sludge

The rheological behaviour of DSS can be effectively modelled using analogue mechanical models, which represent complex flow, deformation, and recovery responses through intuitive combinations of idealized mechanical elements: springs (elasticity), dashpots (viscosity), and friction sliders (yield stress) [124,125]. These models provide physical insight into DSS behaviour during handling, pumping, and processing operations [27,126,127]. Figure 2 presents the hierarchical progression from single-element fundamentals, through two-element viscoelasticity, three-element consolidation and relaxation, culminating in the comprehensive four-element Burgers model.

Figure 2a illustrates the simplest rheological element, the Hookean spring representing instantaneous, fully reversible elasticity. Under applied stress σ, the solid undergoes proportional deformation $\varepsilon = \sigma / E$, where E is the elastic modulus characteristic of the solid. Upon stress removal, complete strain recovery occurs instantly with no time-dependency.

The Newtonian dashpot, shown in Figure 2b, represents pure viscous flow without elastic recovery. Applied shear stress $\frac{d\sigma}{dt}$ produces a steady-state shear rate $\frac{d\varepsilon}{dt} = \frac{\sigma}{\eta}$, where η is the constant viscosity.

Figure 2c shows the friction slider (Bingham element), representing yield stress behaviour characteristic of structured materials. Below critical yield stress σ_c (friction block locked), no deformation occurs ($\sigma = 0$). Above σ_c, the slider unlocks, enabling plastic irreversible deformation $\sigma = \sigma_c$.

The Maxwell model, shown in Figure 2d, combines a spring (E) and dashpot (η) in series to represent viscoelastic fluid behaviour with stress relaxation. Total strain is the sum of elastic $\varepsilon = \sigma E$ and viscous $\frac{d\varepsilon}{dt} = \frac{\sigma}{\eta}$ components. During a creep test, where σ = constant = σ_0, the Maxwell model gives $\varepsilon = \frac{\sigma}{E} + \frac{\sigma t}{\eta}$.

Figure 2e illustrates the Kelvin–Voigt model, featuring a spring (E) and dashpot (η) in parallel to represent retarded elasticity. Both elements share identical strain $\frac{d\varepsilon}{dt}$, but equal stress partitions $\sigma = E\varepsilon + \eta\frac{d\varepsilon}{dt}$. Under constant stress σ_0, strain approaches equilibrium asymptotically to $\varepsilon = E\sigma_0\left(1 - e^{-\frac{E}{\eta}t}\right)$.

Figure 2f depicts the Bingham model, consisting of a friction slider (critical yield stress σ_c) in series with a Newtonian dashpot (plastic viscosity η_p). Below σ_c, the slider remains locked (no flow: $\frac{d\varepsilon}{dt} = 0$). Above σ_c, flow initiates following $\sigma = \sigma_c + \eta\varepsilon$ with permanent plastic deformation with no elastic recovery.

The Terzaghi–Voigt model is described in Figure 2g, extending Kelvin–Voigt viscoelasticity with series elastic compliance. A Voigt element ($E_1 \parallel \eta$) in series with spring or Terzaghi element E_2 captures both instantaneous elasticity ($E_1 + E_2$) and retarded viscous response through dashpot η. The stress equation can be expressed as $\sigma = (E_1 + E_2)\frac{d\varepsilon}{dt}$.

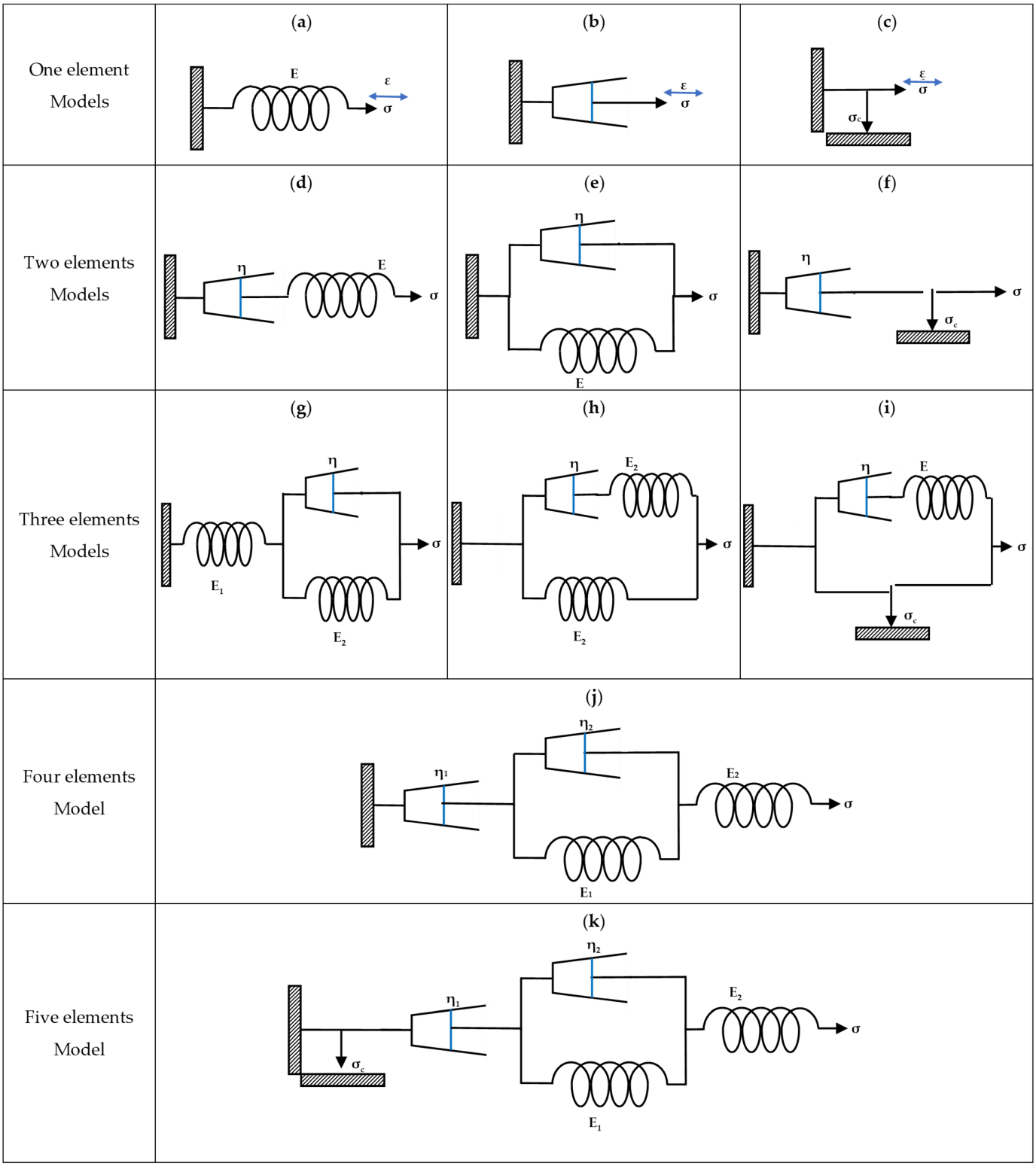


Figure 2. Hierarchical mechanical–analogue rheological models for characterizing DSS. (**a**) Hookean spring Model (Ideal elastic solid). (**b**) Newtonian dashpot Model (Ideal viscous liquid). (**c**) Friction slider Model (Ideal frictional solid). (**d**) Maxwell Model. (**e**) Kelvin-Voigt Model. (**f**) Bingham Model. (**g**) Terzaghi-Voigt Model. (**h**) Zener Model. (**i**) Bingham-elastic Model. (**j**) Burgers Model. (**k**) Burgers-Ludwik Model.

The Zener model (Standard Linear Solid) is shown in Figure 2h, comprising spring E_2 alone in parallel with a Maxwell arm ($E_1 - \eta$). This configuration yields partial stress

relaxation with the equilibrium modulus $E_{eq} = E_1 + E_2$. The stress–strain relation is $\sigma + \lambda \frac{d\sigma}{dt} = E_0\varepsilon + \eta \frac{d\varepsilon}{dt}$, where relaxation time $\lambda = \frac{\eta}{E_1}$ and $E_0 = \frac{E_1 E_2}{E_1+E_2}$.

The elasto-viscoplastic Bingham model is presented in Figure 2i with additive strain decomposition $\varepsilon = \varepsilon^e + \varepsilon^p$. Elastic strain ε^e follows Hooke's law ($\sigma = E\,\varepsilon^e$), while viscoplastic strain ε^p activates above yield σ_c following Bingham flow $\varepsilon^p = \frac{\sigma-\sigma_c}{\eta}$ for $\sigma > \sigma_c$ or $\varepsilon^p = 0$ for $\sigma < \sigma_c$.

The Burgers model, shown in Figure 2j, associates the Maxwell ($E_1 - \eta_2$) and Kelvin–Voigt ($E_2 \parallel \eta_1$) models in series. It models irrecoverable and delayed deformations due to the viscous effects of the material, serving also as a quantitative model for polymer behaviours. Its essential advantage lies in simultaneously presenting relaxation and creep phenomena within a single product, combining instantaneous elasticity ($E_1 + E_2$) delayed elastic recovery (Kelvin arm), permanent viscous flow (η_1), and retarded viscous dissipation (η_2).

Finally, the Burgers–Ludwik model shown in Figure 2k extends the Burgers configuration by including additional nonlinear elements to capture strain hardening or rate-dependent viscosity, enabling a more comprehensive representation of complex sludge rheology.

Taken together, the hierarchical organization of rheological, textural, and viscoelastic models highlights both the diversity of approaches and the increasing complexity required to accurately describe dewatered sewage sludge behaviour. However, beyond their theoretical formulation, it is equally important to understand how these models have been adopted and evolved within the scientific community. In this context, a bibliometric analysis provides valuable insights into research trends, influential contributions, and mapping networks in the field.

6. Literature Review Strategy

A systematic search was performed in five stages as proposed in the literature [128,129]. The main steps are as follows:

1. **Identification of the need for information (sources and access):** The scope of the information need and the relevant domain of knowledge were first defined. The study focused exclusively on scientific contributions (SCs) addressing sludge rheology. Scopus® and Web of Science® were selected as the primary data sources, as they are widely recognized as the most comprehensive and reliable databases for chemical and environmental engineering, encompassing more than 95% of the scientific literature [130,131].
2. **Planning:** A search equation was proposed ("sludge" AND "rheology") to describe the field with no restrictions.
3. **Search and processing of information:** Searches were performed in the "Title–Abstract–Keywords" field in Scopus® and in the "Topics" field in Web of Science®, which serves an analogous function.
4. **Analysis and enhancement of the information:** The bibliographic dataset was analyzed using the following tools and procedures.
    (a) **Tree of Science** [132] was used to classify documents as roots (seminal works), trunks (core contributions forming the backbone of knowledge in the field), branches (describing recent research lines), and leaves (newest contributions in the field). This classification supported the qualitative evaluation of the literature and facilitated assessment of the intellectual structure of the field.
    (b) **Bibliometrix®**, 5.0 an R package for bibliometric analysis [133], was employed to remove duplicates and generate a single, cleaned database. The package provides advanced analytical and categorization capabilities, surpassing those of CiteSpace® 7.0 and VOSViewer® (version 1.6.20) for certain tasks [134].

(c) Although Bibliometrix® enables the construction of bibliometric networks (e.g., keyword co-occurrence or citation networks), its visualization capabilities are limited. Therefore, networks were computed using Bibliometrix® and subsequently exported to **VOSViewer®** for enhanced visualization. VOSViewer® is a dedicated tool for constructing and visualizing bibliometric networks and includes text-mining functionalities [135,136].

(d) **Export to Python.** Selected outputs from Bibliometrix® were exported as numerical arrays and further processed, analyzed, and visualized using Python 3.14 to improve the clarity and customization of graphical representations.

(e) **Field clean up and standardization.**

i. Author-provided keywords are inherently heterogeneous, as different terms may be used to describe identical or closely related concepts. To address this issue, keywords were analyzed, catalogued, and consolidated through the construction of a thesaurus of synonyms, enabling more accurate identification of thematic trends.

ii. Author affiliations were standardized, as institutional names were sometimes reported inconsistently or in different languages across publications.

iii. Author disambiguation was performed to mitigate errors arising from identical surnames and initials, which can compromise automatic counting and attribution procedures.

5. **Results report and communication:** Processed data is organized, analyzed and key findings are reported to the scientific community.

Steps 2 through 4 were repeated iteratively, as new keywords were added to the search equation, which enhances the quality of the search as the initial equation might omit important terms [137–139]. The iterative process was stopped once the top 10 authors, the top 10 journals, and the total number of retrieved documents exhibited changes of less than 5% with respect to the previous iteration as proposed for bibliometric studies [137].

7. Bibliometrics Results

The bibliometric results will be presented in five subsections: First, an overview of the field is provided, highlighting general characteristics and the most influential sources. Next, leading contributions and authors are examined using impact metrics such as local and global citations for publications, and the h-index and g-index for authors, followed by an analysis of author collaboration patterns. The intellectual structure of the field is then explored through a detailed examination of author keywords. The last subsection addresses the social structure of the research area, identifying the most productive countries and institutions and mapping international collaboration networks. A Supplementary File is provided with the SCs included in the analysis. Table S1 presents the keywords and their identified synonyms for disambiguation.

7.1. Main Characteristics

From step 3 of the workflow, 1559 SCs were found, with 999 coming from Scopus and 561 from Web of Science. After using the Tree of Science® and Bibliometrix® tools for removing duplicates, there were a total of 1132 unique documents. A manual inspection revealed no more duplicates. A total of 93% of the documents are written in English, with the remaining 7% written in languages such as: Chinese, German, French, Czech, Spanish, Polish, Japanese, among others.

The SCs were published in 367 different sources (journals, books, conference proceedings), with 2710 different authors, presenting 12.4% international co-authorship. A total of 82% of the documents are articles, 13.6% are conference papers and the remainder are a

mix of reviews and book chapters. The analyzed works span the period from 1961 to 2026, with the field exhibiting an average annual growth rate of 3.61%.

SCs over the years: (a) shows the number of articles published each year and the mean number of citations each article received; (b) presents the cumulative publications in the field and the average citations each article received when divided by year. Figure 3 presents several indicators of the annual scientific contributions. At the top is the published contributions each year with the total citations they have received. As seen, the field was initiated around 1961 with a work focused on obtaining a mathematical model to describe the relationship between shear rate and shear stress for digested SS [140]. The field stayed dormant, with papers published before 2000 comprising less than 10% of the total number of contributions. Moreover, since the early 2000s, the number of publications has risen sharply, as seen at the bottom of Figure 3. This increased interest from the scientific community might have been driven by the publication of the United States' Environmental Protection Agency guidelines to comply with local regulations [140] and several European regulations from 1991 through 2001 [141–144].

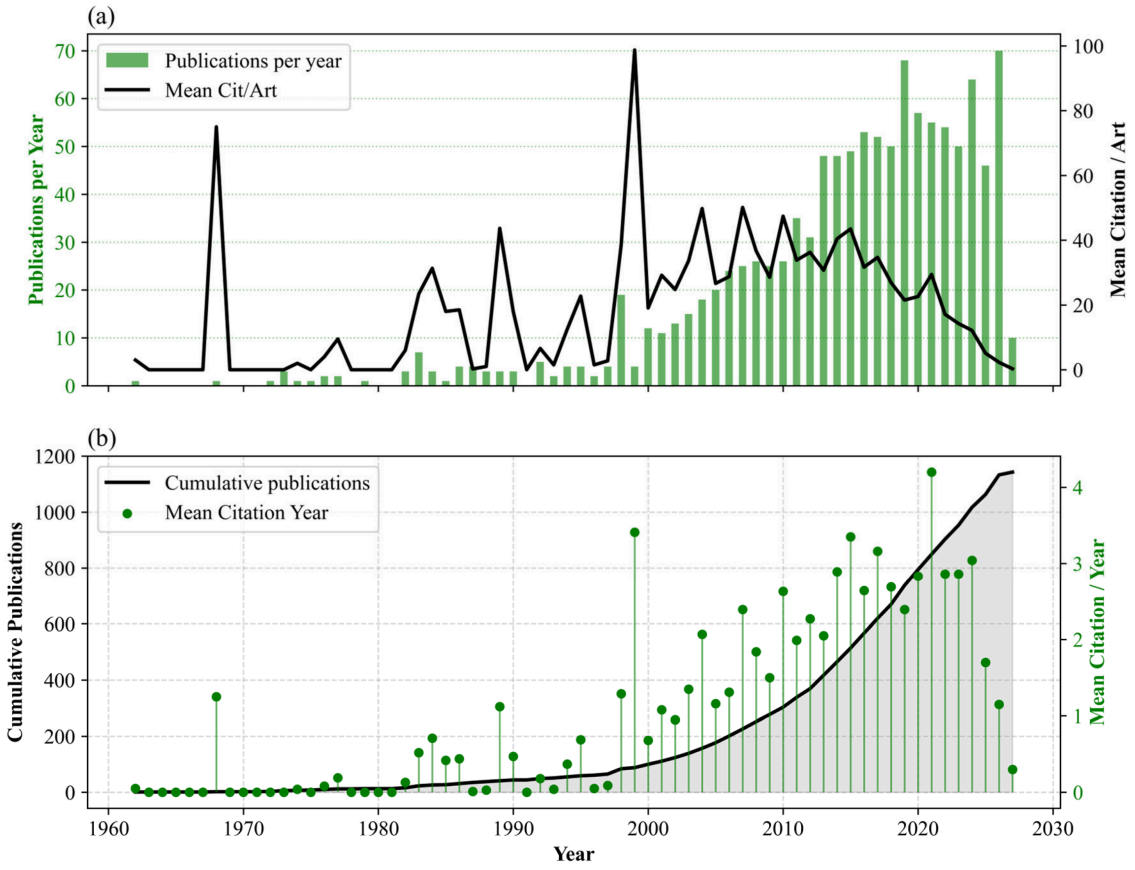


Figure 3. SCs over the years: (**a**) shows the number of articles published each year and the mean number of citations each article received; (**b**) presents the cumulative publications in the field and the average citations each article received when divided by year.

On the other hand, when analyzing the mean citations per article (black line, top Figure 3) the biggest peak is seen in the year 1998 due to the publication of several seminal articles [145–147], while the second peak is from 1967's only paper [148]. However, once the average citations are normalized per year (green lollipops in the bottom of Figure 3), it is seen that SCs have more or less the same values, and that recent works have been more impactful.

The life cycle of a research field is a bibliometric concept describing the temporal evolution of a scientific domain, typically modelled as a logistic S-curve that progresses through emergence (slow initial growth), exponential expansion (rapid knowledge accumulation), and saturation (maturation as core problems are solved) [149–151]. Figure 4 presents the life-cycle analysis for the research field, which has good fit with the proposed model (r^2 = 0.999). As visualized in Figure 4a, the field underwent a prolonged latency phase prior to the year 2000, characterized by sporadic output, before entering a period of exponential expansion that defined its "golden age" of discovery. This rapid accumulation of knowledge culminated near the inflection point (September 2021), which aligns closely with the peak annual production observed in Figure 4b (around March 2021). Currently, the dynamics suggest the field has already undergone its maximum growth velocity and is transitioning into a maturity or saturation phase, approaching a theoretical saturation constant of approximately 1909 publications (which could happen around 2058). This deceleration implies that while the domain remains active, the era of explosive growth has concluded, likely shifting the community's focus from foundational exploration to consolidation and specialized application.

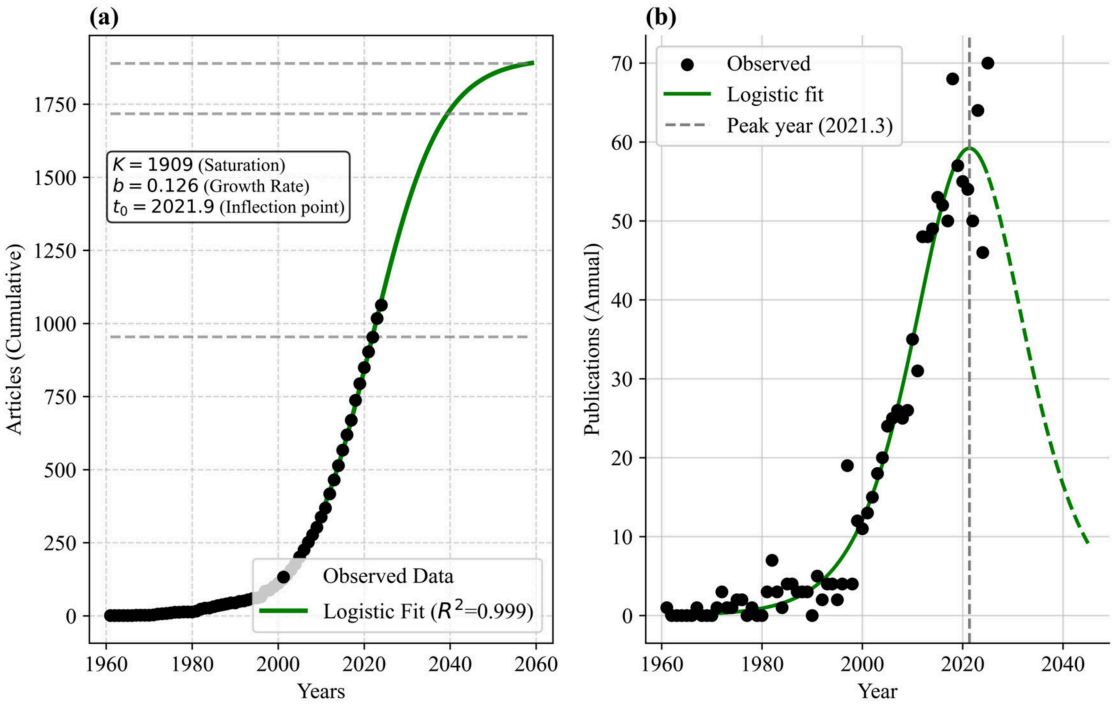


Figure 4. Bibliometric life-cycle analysis of the research field. (**a**) Cumulative growth of scientific production fitted to a logistic model illustrating the saturation capacity (K = 1909), 50%,90 and 99% of the saturation capacity (dashed lines), growth rate (b = 0.126), and the inflection point (t_0). (**b**) Annual publication dynamics comparing observed frequencies (dots) with the logistic derivative curve (solid line), identifying the transition from exponential growth to a post-peak maturity phase around the year 2022 (dashed line).

Table 2 presents the number of publications, the total citations, h and g indexes and the number of publications for the top 6 sources in the field. *Water Research* is the source with the largest number of contributions and total citations, accounting for more than 11% of the contributions in the area. Interestingly, despite being the top journal with less contributions and total citations, publications in *Biochemical Engineering Journal* receive an average of 41.75 citations, making it the journal with the third highest average citations in the field.

Table 2. Top sources by h index, g index, total citations and number of publications.

Source	Editorial	h Index	g Index	Total Citations	Number of Publications
Water Research	Elsevier	47	77	6257	106
Bioresource Technology	Elsevier	34	53	2972	64
Water Science and Technology	IWA	23	42	1963	73
Chemical Engineering Journal	Elsevier	20	28	1066	28
Science of the Total Environment	Elsevier	13	21	548	21
Biochemical Engineering Journal	Elsevier	11	16	668	16

To capture the most influential sources, Bradford's law describes the core journals of a research field, by classifying sources according to their productivity [152,153]. Figure 5 presents Bradford's law for the analyzed sources, showing that the journals listed in Table 1 constitute the core set of publications. *Zone 1* corresponds to the core journals which together account for 31% of the total scientific output. *Zone 2* comprises journals with intermediate productivity, publishing more than three but fewer than eight contributions, and represents approximately 32% of the publications. Taken together, these two zones encompass over 60% of the total output, indicating that the majority of SCs are concentrated within only 74 out of the 367 sources.

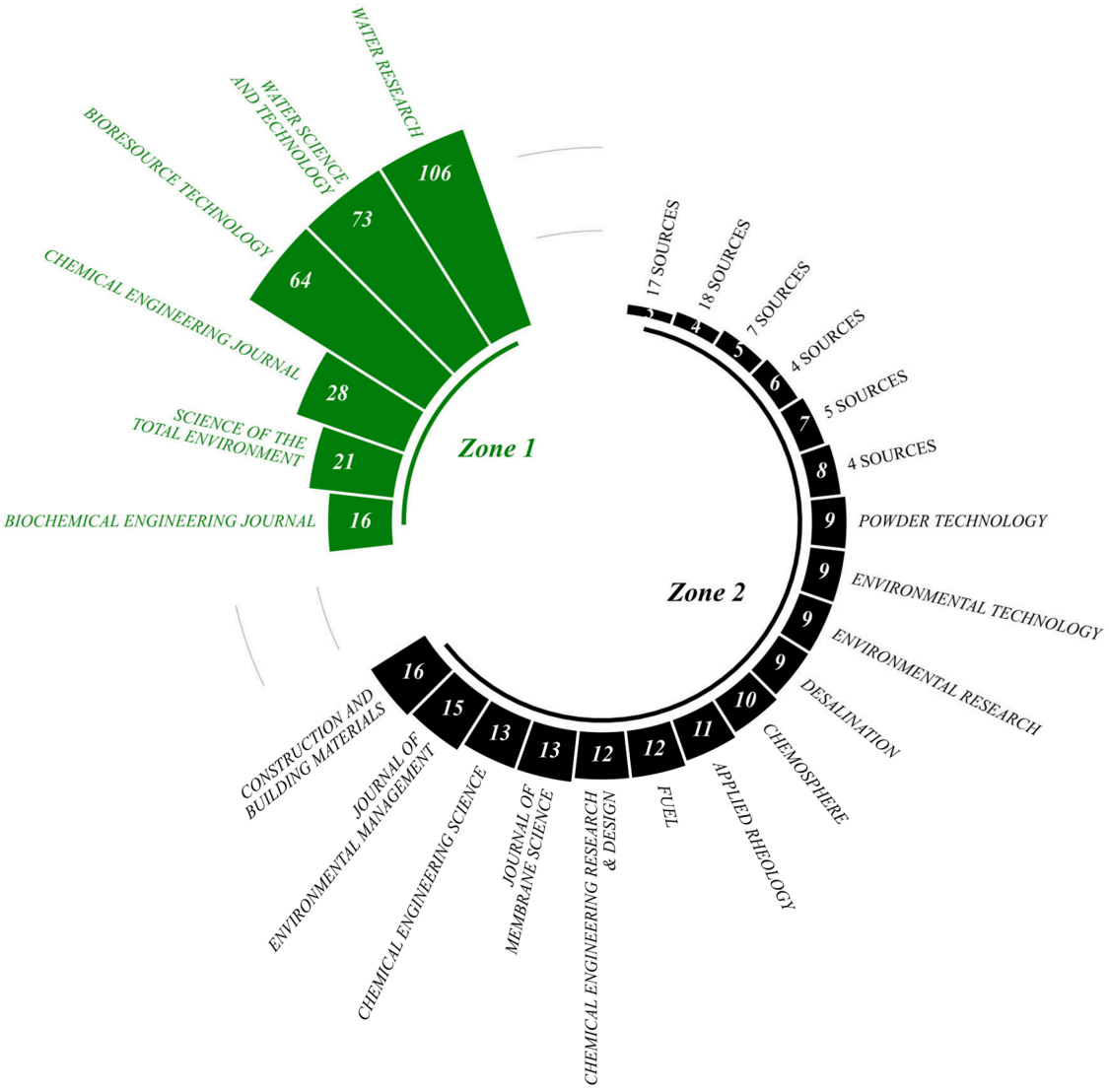


Figure 5. Bradford's law for the different sources.

7.2. Most Relevant Contributions

Table 3 presents the most impactful contributions by total citations and citations per year. These works include reviews on treatment and rheology of SS [29,30,154,155], as well as experimental studies investigating different treatment possibilities such as microwave irradiation [156]; using iron ions to enhance dewaterability [157]; investigating thermal, ultrasonic and ozone pre-treatments to enhance biodegradability [158]; and measuring rheological properties of different EPS forms in activated SS [147] or soybean-processing wastewater [159].

Table 3. Most impactful contributions by total citations and average citations per year.

Title	Reference	Total Citations	Citations per Year
How microorganisms use hydrophobicity and what does this mean for human needs?	[154]	561	43.15
Effect of ultrasonic, thermal and ozone pre-treatments on waste activated sludge solubilisation and anaerobic biodegradability	[158]	491	23.38
Thermal hydrolysis for sewage treatment: A critical review	[155]	365	33.18
Formation and Characterization of Aerobic Granules in a Sequencing Batch Reactor Treating Soybean-Processing Wastewater	[159]	288	13.09
Hydrophobic/hydrophilic properties of activated sludge exopolymeric substances	[147]	271	9.34
Rheological characterisation of municipal sludge: A review	[14]	234	33.43
Fe(II) catalyzing sodium percarbonate facilitates the dewaterability of waste activated sludge: Performance, mechanism, and implication	[157]	227	16.21
Microwave-acid pretreatment: A potential process for enhancing sludge dewaterability	[156]	215	19.55
State-of-the-art: rheological characterisation of wastewater treatment sludge	[30]	210	8.75
Activated sludge rheology: A critical review on data collection and modelling	[29]	202	14.43

Interestingly, the two most cited works [154,158] are not present in the Core Journals identified in Zone 1 of Bradford's law, instead being published in *Frontiers in Cellular and Infection Microbiology* and *Chemical Engineering and Processing: Process Intensification*, respectively.

7.3. Authors' Analysis

Table 4 shows the most impactful authors by g-index, h-index, total citations, number of publications, and average citations per document. Nicky Eshtiaghi is the author with the greatest number of publications and total citations, and highest h and g indexes. However, he is the fourth most impactful author when measured by the average citations of their documents. Moreover, despite having less publications, Slatter P.T, Surampalli Rao, and Brar Satinder present high average citations per document, indicating the higher local impact of their SCs.

Figure 6 shows the co-citation network for the top 50 authors most cited. Three different clusters can be identified, with the authors mentioned in Table 4 taking a central role in bridging connections between different clusters. As expected, Jean Cristophe Baudez (in red) and Nicky Esthiaghi (in green) are the biggest nodes in the network, indicating that they are highly influential in the research field.

Table 4. Most impactful authors.

Author	h Index	g Index	Total Citations	Number of Publications	Average Citations per Document
Eshtiaghi Nicky	21	40	1644	43	38.2
Baudez Jean Christophe	21	38	1562	38	41.1
Slatter P. T.	15	20	1106	20	55.3
Surampalli Rao Y.	11	12	657	12	54.8
Brar Satinder K.	11	12	635	12	52.9
Dentel Steven K.	16	17	567	17	33.4
Lee Duu-Jong	11	15	514	15	34.3
Parthasarathy Rajarathinam	12	18	510	18	28.3

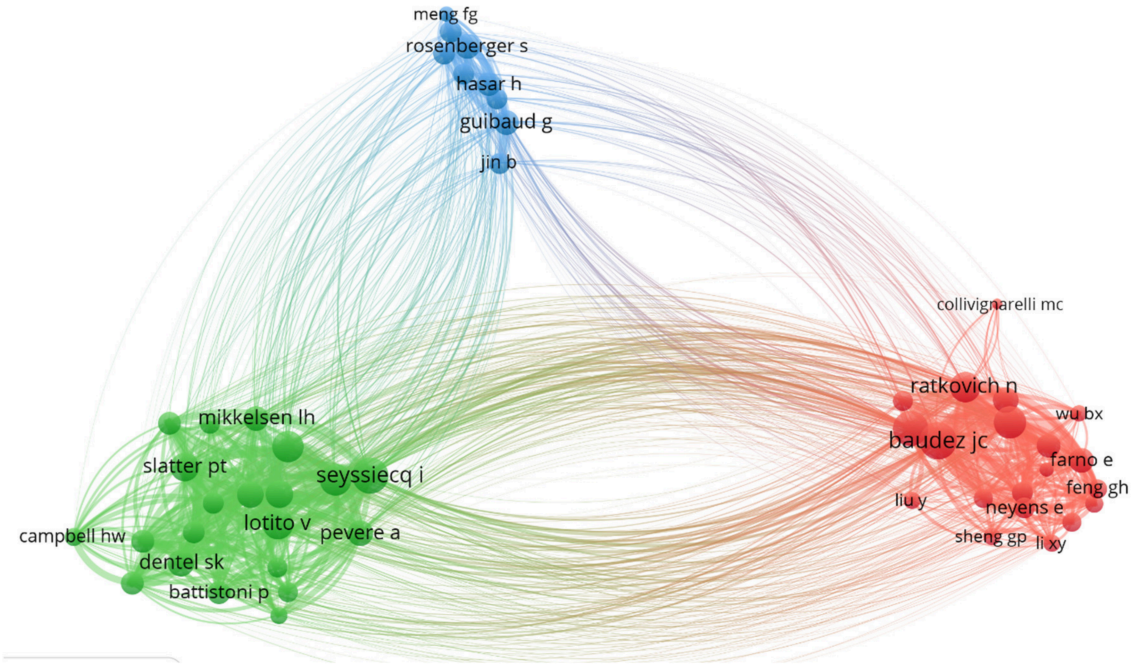


Figure 6. Co-citation network for the field. Different colours represent different clusters of authors being co-cited together.

7.4. Keywords Analysis

Figure 7 presents the top 20 most used authors' keywords. The most used keywords are "sludge" (1006 occurrences) and "rheology" (966 occurrences), suggesting the field has focused on the mechanical behaviour and flow properties of complex biological suspensions, supported by the presence of technical parameters like "viscosity", "yield stress", and "flow kinetics". This core thematic cluster is supported by secondary focus areas in "wastewater treatment" (447) and "polymer" (289) science, indicating interest for optimizing treatment processes through chemical and physical interventions. The use of "computational fluid dynamics" suggests efforts for mathematical modelling of non-Newtonian fluids to enhance bioreactor efficiency and SS dewatering technologies.

Figure 8 shows the keyword co-occurrence network. The co-occurrence network analysis reveals a highly interconnected scientific structure characterized by two primary thematic clusters that bridge fundamental rheology with process engineering. Cluster 1 (in red) represents the "Methodological Core," anchored by nodes "rheology" and "sludge". Auxiliary terms like "yield stress" and "viscosity" connect the main topics to operational factors such as "anaerobic digestion" and "suspensions." This suggests that rheological

characterization is the fundamental lens through which SS behaviour is interpreted, connecting to Cluster 2 (blue), which mainly contains some techniques used for characterizing SS like "dewatering", "adsorption", "and "particle size".

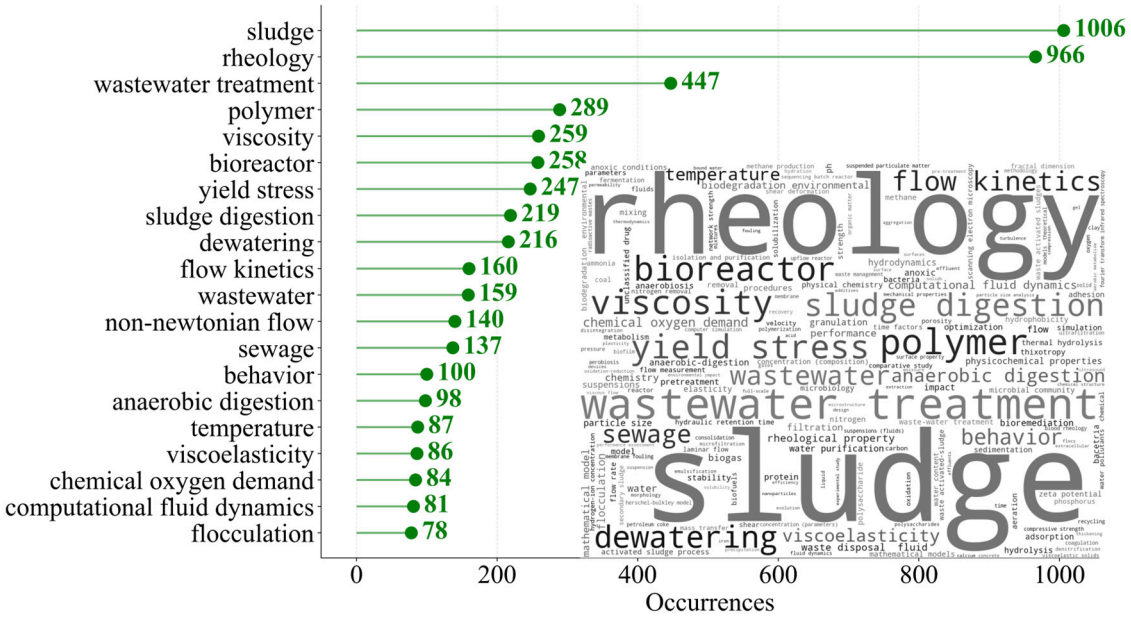


Figure 7. Top 20 keywords by number of occurrences and Wordcloud with 200.

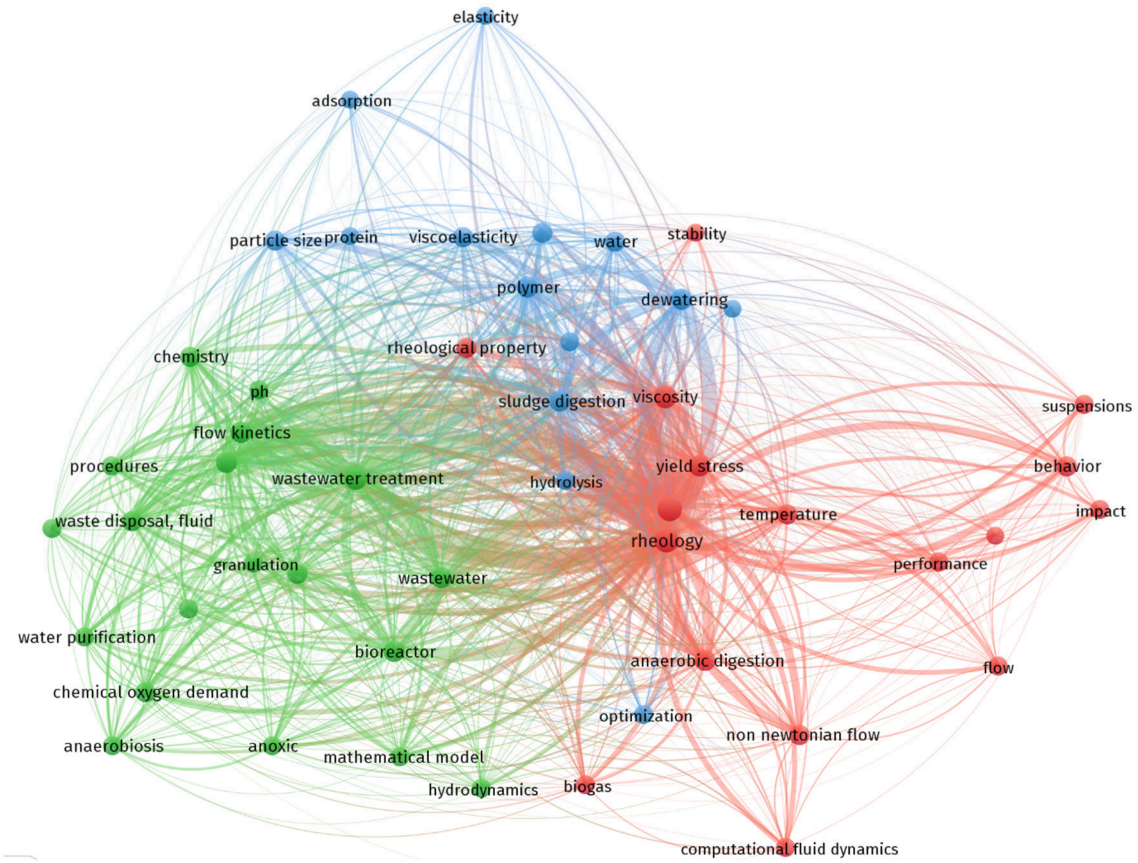


Figure 8. Keyword co-occurrence network.

In contrast, Cluster 3 (green cluster) functions as the "Application-Driven Domain," focusing on the kinetics and efficiency of treatment infrastructures. Cluster 2's primary

elements like "wastewater treatment", "wastewater", "waste disposal", "water purification" and "bioreactor" link to potential industrial applications, especially considering the connection to "computer fluid dynamics" from Cluster 1.

Figure 9 presents the thematic evolution of the field, separated in time slices containing an equal number of scientific contributions. This evolution reveals a progressive transition from general bioprocess observations toward highly specialized rheological modelling. In the early periods (1961–2007), research was primarily focused on bioreactor behaviour and mathematical modelling, whereas from 2009 through to 2018 the field shifted towards rheology and wastewater treatment as central themes driving innovation. Since 2019, "sludge", "wastewater treatment" and "rheology" have once again become the motor themes of the field, signalling consolidation towards applications.

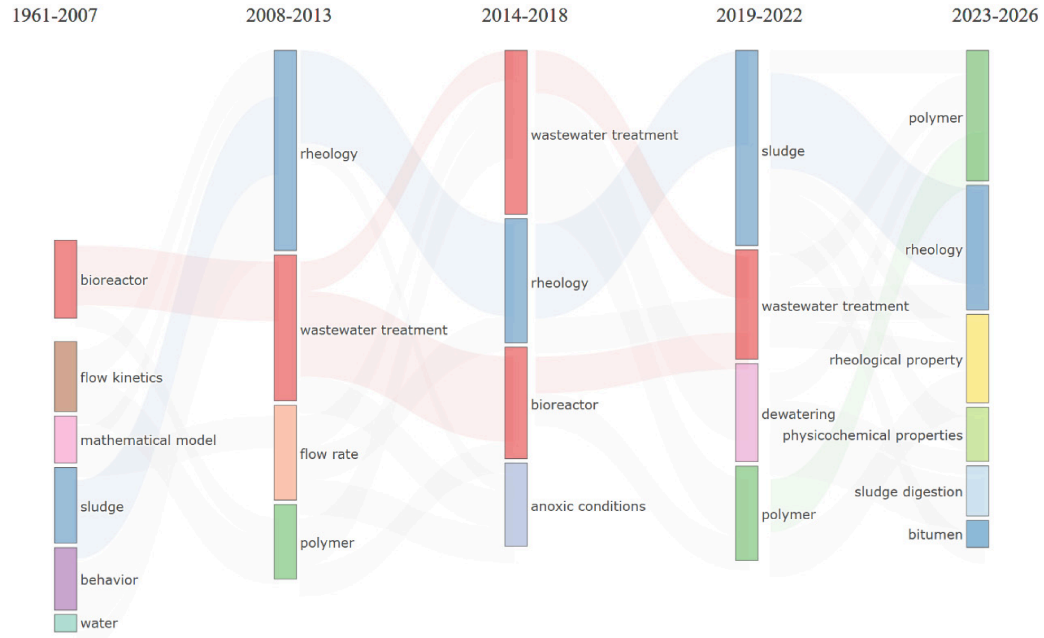


Figure 9. Thematic evolution.

In the most recent era (2019–2026), the field exhibits significant thematic branching, where the central "sludge" node has given rise to specialized sub-domains such as "sludge digestion", "physicochemical properties" and "polymer" science. Modern research trajectories now integrate complex techniques like "computational fluid dynamics (CFD)", showing interest in applying mathematical modelling to enhance operational sustainability of global wastewater infrastructures.

7.5. International Collaboration

The analysis of global scientific production reveals a highly stratified landscape dominated by a few key nations. China emerges as the primary contributor with 484 publications, significantly outperforming other high-output countries such as the USA (152), Australia (145), and France (142). Collectively, these four nations account for approximately 51% of the total scientific output (1797 publications). These nations, alongside Italy (77 publications) and Germany (53 publications), face medium to high water risk and scarcity [160], which might explain the interest for researching sludge treatment technologies and techniques.

Figure 10 presents the map of scientific collaboration. This map underscores the importance of strategic bilateral partnerships in advancing scientific knowledge. USA and Canada are the countries with the highest number of collaborations (15). Other significant nodes of interaction include Australia's robust connections with France (11) and the United

Kingdom (5), as well as the USA's emerging link with Turkey (8). Despite the high volume of independent production in China, the collaboration data suggests that Western nations currently maintain more integrated and high-frequency cross-border research pipelines, which has been seen in other fields [161].

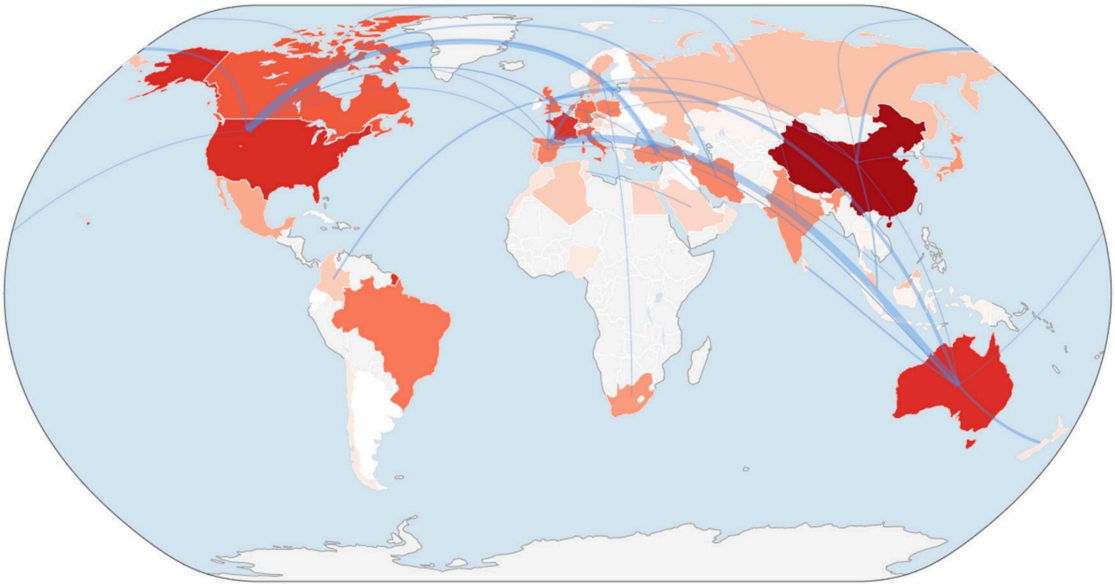


Figure 10. Country collaboration map.

The bibliometric analysis of authors' keywords provides a coherent framework to contextualize the structure of this review by revealing both the dominant research axes and the existing gaps in the field. The prevalence of the term *sludge* (although inherently influenced by the search strategy) highlights the necessity of establishing a clear and rigorous definition of sewage sludge and its transformation along the treatment line, which is addressed in Section 4. Furthermore, the strong prominence of rheology-related terms confirms that the mechanical behaviour of sludge constitutes a central research focus, thereby justifying the inclusion of Sections 5 and 6, where rheological, textural, and viscoelastic modelling approaches are systematically presented to interpret and predict sludge behaviour under operational conditions. In alignment with this modelling perspective, the presence of keywords associated with characterization techniques supports the development of Sections 7 and 8, dedicated to experimental methods for assessing mechanical and rheological properties. Finally, the absence of terms such as *adhesion* in the keyword landscape reveals a critical blind spot in the literature. Finally, the absence of terms such as adhesion in the keyword landscape reveals a critical blind spot in current research. This omission underscores the importance of Section 9, which specifically addresses adhesiveness as an overlooked yet significant property in sludge mechanical characterization.

8. Experimental Methods for Mechanical and Rheological Characterization of Dewatered Sewage Sludge

From the literature bibliometrics results, a wide variety of experimental techniques have been employed to characterize the rheological, textural and geotechnical behaviour of DSS. These methods originate from different disciplines, classical rheometry, food texture analysis, soil mechanics or empirical consistency testing; and are therefore based on distinct loading modes, measurement principles and data reduction procedures. In the following, the main tests reported for DSS are described in a systematic manner, detailing their

physical working principle, measured variables, historical origin and main strengths and weaknesses when applied to DSS.

For clarity and consistency throughout this review, the following terminology will be used. The terms adhesion and cohesion are employed when referring to the physical phenomena and interfacial or internal interactions in a general sense. The terms adhesiveness and cohesiveness are used when referring to the corresponding parameters measured by textural or empirical tests, such as penetration, texture profile analysis, and uniaxial compression, where probe detachment, structural recovery, or internal resistance are evaluated. When a method directly measures a force or resistance, the specific technical term associated with that test is preferred, such as adhesive force in probe-based or pull-off methods, detachment force in surface adhesion tests, shear strength in direct shear, triaxial, vane shear, or unconfined compression tests, and yield stress in rheological or slump-based methods. This terminology is intended to improve readability, avoid ambiguity, and facilitate comparison among the different experimental methods discussed in this review.

8.1. Atterberg Limit Tests

The Atterberg limit tests were originally developed by Albert Atterberg in 1911 to classify fine-grained soils and clays according to their consistency and plasticity range [162], initially defining seven qualitative limits: upper viscous flow limit, lower viscous flow limit), sticky limit, rolling limit, cohesion limit, water tightness limit, and shrinkage limit. They are based on the empirical observation that cohesive materials undergo a progressive transition from a liquid to a plastic and finally to a semi-solid state as water content decreases. In their classical form, rationalized by Casagrande [162,163], the tests determine three characteristic water contents: the liquid limit (L), the plastic limit (PL), and less frequently the shrinkage limit (SL), which delimit these consistency states and allow the computation of simple plasticity indices $(PI = LL - PL)$ [163].

The LL can be measured using two standardized methods: the Casagrande cup method and the cone penetrometer method. The Casagrande cup method involves the use of standardized equipment to ensure consistent measurement (ASTM D4318) [164]. Basically, the test consists of spreading a sludge sample in a standard-size cup and then cutting a groove in the centre. The cup is dropped repeatedly and the number of blows required to close the groove is measured. Once the groove has closed, the water content of the sample is measured at 105 °C [165].

The procedure is repeated at several different water contents. The number of blows is plotted against water content on a semi-logarithmic graph, and the liquid limit is obtained by interpolation as the water content corresponding to 25 blows. The Casagrande cup apparatus is shown in Figure 11a, and a typical representation of the test results is presented in Figure 11b.

The cone penetrometer method (ASTM D3441-16) [166], preferred for its superior reproducibility, employs a standardized stainless-steel cone (80 g mass, 30° apex angle, specific height). Sludge samples at varying water contents are tested by releasing the cone to fall freely for 5 s onto the sample surface, with penetration depth recorded immediately after; results are plotted (penetration vs. water content in a semi-logarithmic graph), and the liquid limit (LL) is determined by extrapolation at exactly 20 mm penetration [167]. The cone penetrometer apparatus is shown in Figure 12a, and the general results obtained from the test are shown in Figure 12b.

Finally, the plastic limit (PL) is determined manually by forming an 8 g sludge patty into a 3 mm diameter thread by rolling it on a ground glass plate until it crumbles longitudinally at a length of 25–30 mm. The sludge must be rolled for at least 2 min at 80–90 strokes per minute; if the thread remains cohesive and the diameter is less than 3 mm after these

strokes, the sludge is still in the plastic state and its water content exceeds the PL. The Figure 13 resumes this experimental method.

In DSS, these tests have been widely applied to characterize plasticity and geotechnical stability [34–36,94,95,168,169]. Reported values indicate that digested sludges tend to exhibit higher plasticity than primary sludges, reflecting differences in organic structure and water retention capacity. Liquid limit (LL) values commonly exceed 80% and may surpass 100% in deeply DSS, whereas plastic limit (PL) values are often reported within the range of approximately 50–90%, leading to elevated plasticity indices [96]. These values are generally higher than those of conventional mineral soils and are strongly influenced by treatment processes and organic fraction.

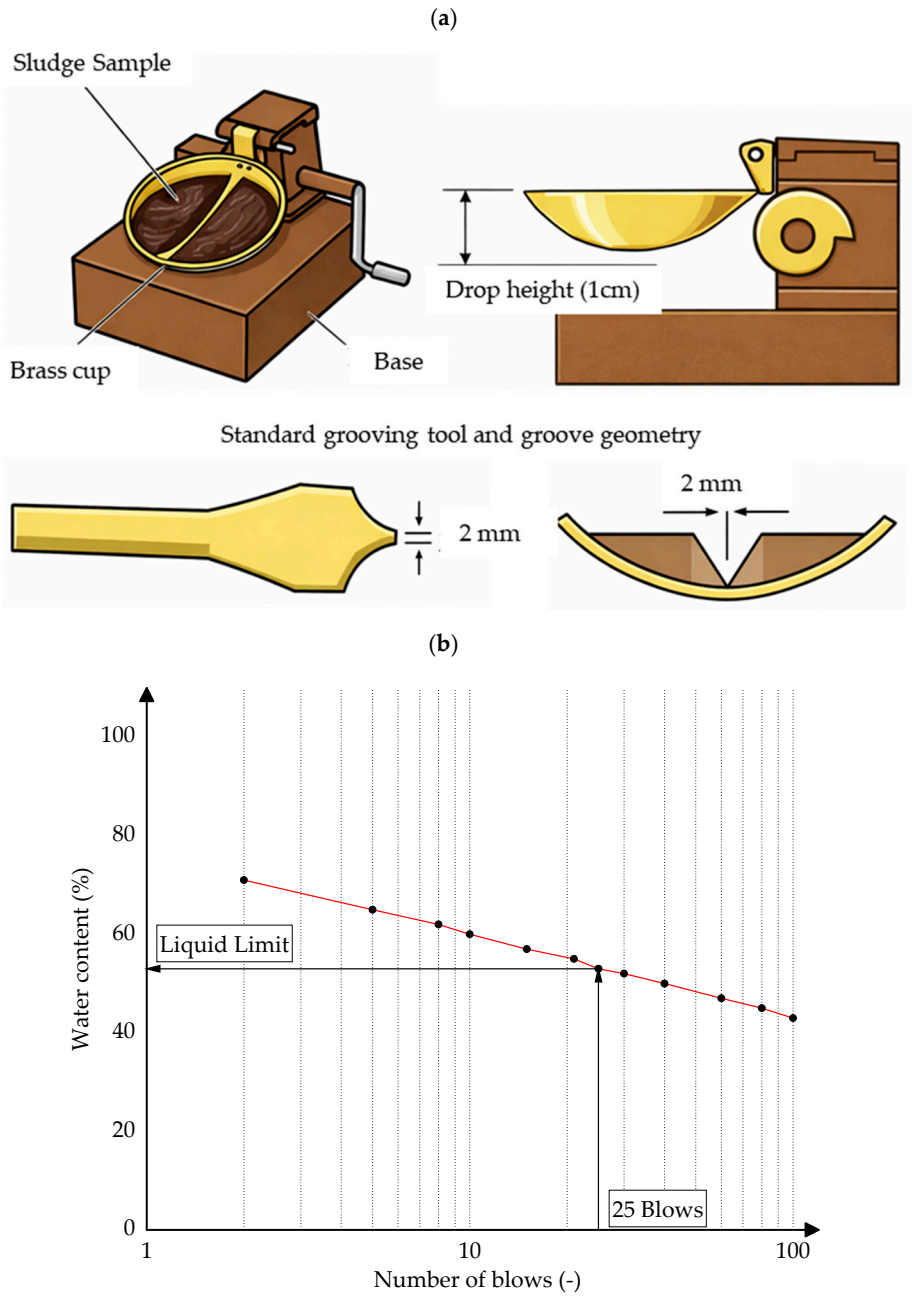


Figure 11. The Casagrande cup method: (**a**) Casagrande apparatus; (**b**) Casagrande classic results.

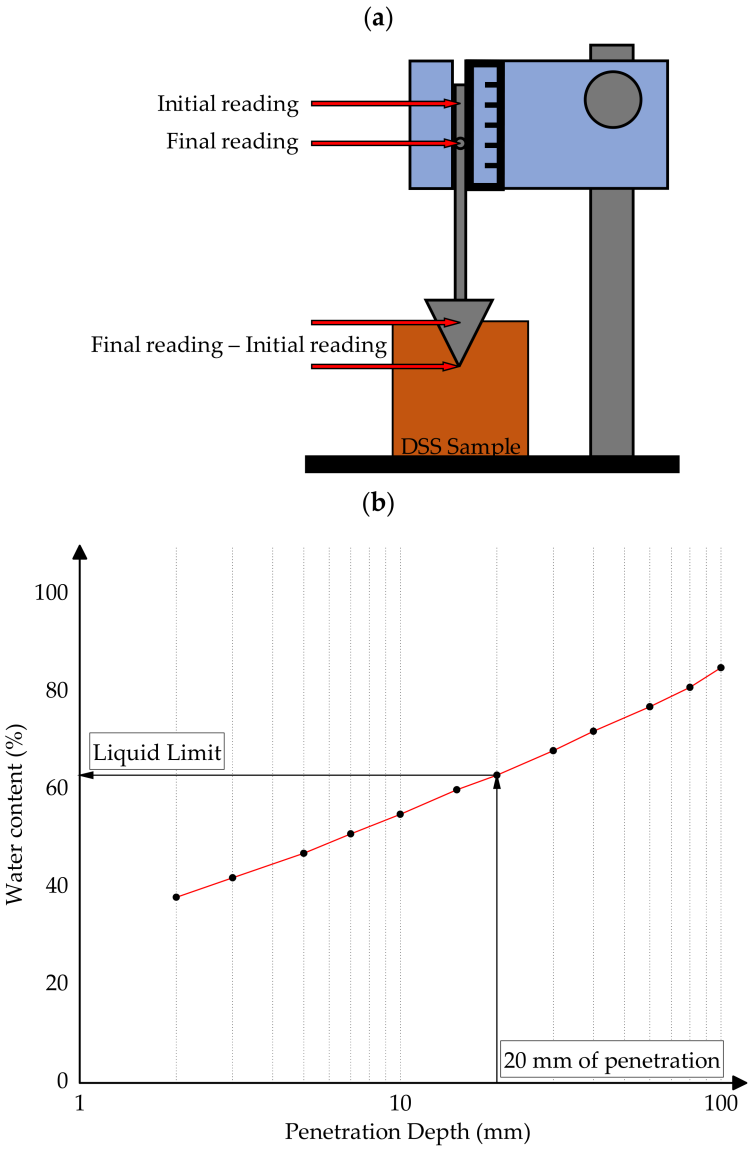


Figure 12. The cone penetrometer method: (**a**) cone penetrometer; (**b**) cone penetrometer classic results.

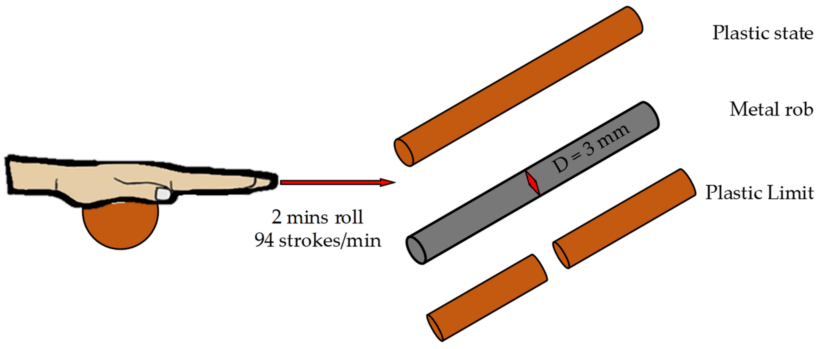


Figure 13. Plastic limit test.

Despite being simple and rapid, Atterberg limit tests present limitations when applied to DSS. Their empirical nature, operator dependence, and sensitivity to organic heterogeneity reduce reproducibility, and the results do not directly represent mechanical behaviour under operational conditions such as pumping or stacking. Therefore, in sludge systems, consistency limits should be interpreted as qualitative indicators of worka-

bility and structural state, best used in conjunction with rheological and strength-based measurements [94,163,167].

8.2. Slump Test

The slump test, originally outlined in British Standard 1881 and now used for assessing the workability and consistency of fresh concrete [170], modelled by Murata [171], has been adapted to characterize the flowability and yield stress of concentrated SS, including DSS, providing a simple empirical index of "solid-like" vs. "fluid-like" behaviour [172].

In its standard form, the test employs a metallic, open-ended, truncated cone (Abrams cone) with a base diameter of 200 mm, top diameter of 100 mm, and height of 300 mm. The cone is placed on a flat, rigid surface and filled vertically with the sludge sample in three or more layers; each layer being lightly tamped to minimize the inclusion of large air voids. Once filled and levelled, the cone is carefully lifted vertically at a controlled speed, allowing the material to deform freely under gravity. The difference between the initial cone height and the final height of the slumped specimen (slump height) is then recorded and used as an index of consistency and yield stress.

To facilitate analytical modelling, Pashias et al. [173] replaced the truncated cone by a right circular cylinder (typically 200 mm in diameter), simplifying the description of the stress distribution and the relationship between slump and yield stress. Building on this framework, Baudez et al. [174] further modified the apparatus by adding a cylindrical hat on top of the sample, on which calibrated masses can be placed, together with a vertical guide axis to ensure purely vertical loading. This adapted configuration, which has been successfully applied to DSS, enables both the conventional slump measurement and the application of additional normal stress to promote controlled collapse of highly cohesive, paste-like materials. A schematic representation of the modified slump test proposed by Baudez et al. is shown in Figure 14.

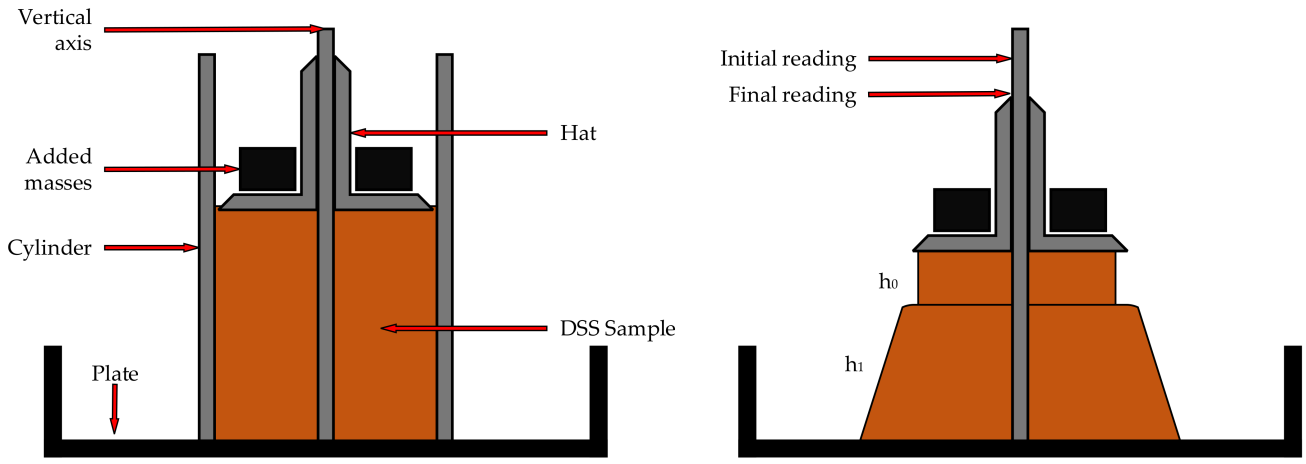


Figure 14. Baudez slum test evolution.

According to the theoretical framework established by Pashias et al. [173] and refined by Baudez et al. [174], the shear stress τ_1 can be calculated from the measured slump height (S) using:

$$S = H - (h_0 + h_1)$$

$$S = H + z_0 - \frac{2\tau_1}{\rho g}\left(1 + \ln\left(\frac{\rho g(H + z_0)}{2\tau_1}\right)\right)$$

with

$$z_0 = \frac{m_0}{\pi \rho R^2}$$

where H, h_0 and h_1 are the initial height.

The method has been successfully applied to SS with solids contents typically ranging between 5% and 15%, where the material exhibits viscoplastic behaviour [172,174,175]. In this range, correlations between slump-derived shear stress and conventional rheometric measurements have shown satisfactory agreement, validating the method as a practical alternative for field and laboratory applications.

The main advantages of the slump test lie in its simplicity, low cost, and suitability for in situ rheological assessment without sophisticated instrumentation. However, its empirical nature, sensitivity to geometry and lifting procedure, and limited applicability at very high solids contents (where structural collapse may be incomplete) restrict its use to moderately concentrated sludge. Therefore, while highly useful as a rapid shear stress indicator, the slump test should be complemented by controlled rheometric measurements when detailed viscoelastic characterization is required.

8.3. Direct Box Shear Test

The direct box shear test or just direct shear test, developed in the early 20th century for soil mechanics and standardized as ASTM D3080 [176], measures the peak shear strength and frictional properties of cohesive or granular materials under controlled normal stress, through the Mohr–Coulomb failure criterion, using undisturbed or remoulded samples confined in a split shear box [177,178].

The sample is placed in a shear box assembly, which includes two metal plates, porous stones, retaining screws, a gripper disk, and a loading cap to apply normal stress. Available in circular or square configurations, the shear box limits the specimen's horizontal deformation while allowing shear failure along the horizontal plane where the plates meet. A schematic of the experimental setup is shown in Figure 15.

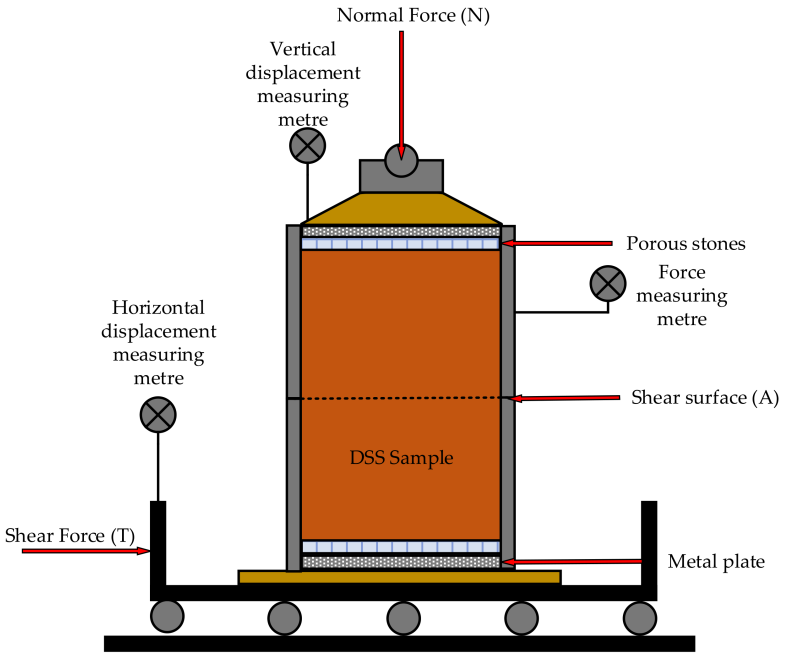


Figure 15. The direct box apparatus.

Figure 16 illustrates the typical results obtained from the direct shear test. For each imposed normal stress ($\sigma_1 < \sigma_2 < \sigma_3$), the shear stress ($\tau$) initially increases with shear displacement until reaching a peak value $\left(\tau_f\right)$, corresponding to failure along the predefined horizontal plane. In some materials, this peak may be followed by strain softening toward a residual shear stress, whereas in more ductile systems the curve may

exhibit gradual strain hardening. The peak shear stress recorded for each applied normal stress is used to construct the Mohr–Coulomb failure envelope. By plotting τ_f versus σ_n, a linear relationship is typically obtained, expressed as:

$$\tau_f = c + \sigma_n \tan(\varphi)$$

where c is the apparent cohesion and φ is the internal friction angle. The intercept of the linear regression with the shear stress axis corresponds to cohesion (c), while the slope of the line equals $\tan(\varphi)$ and σ_n is the normal effective stress (σ_n). These parameters describe the shear strength of the material under drained conditions and are fundamental for geotechnical stability calculations, including slope stability and bearing capacity analyses. The test therefore allows the mechanical characterization of DSS in terms of their resistance to shear under controlled normal loading.

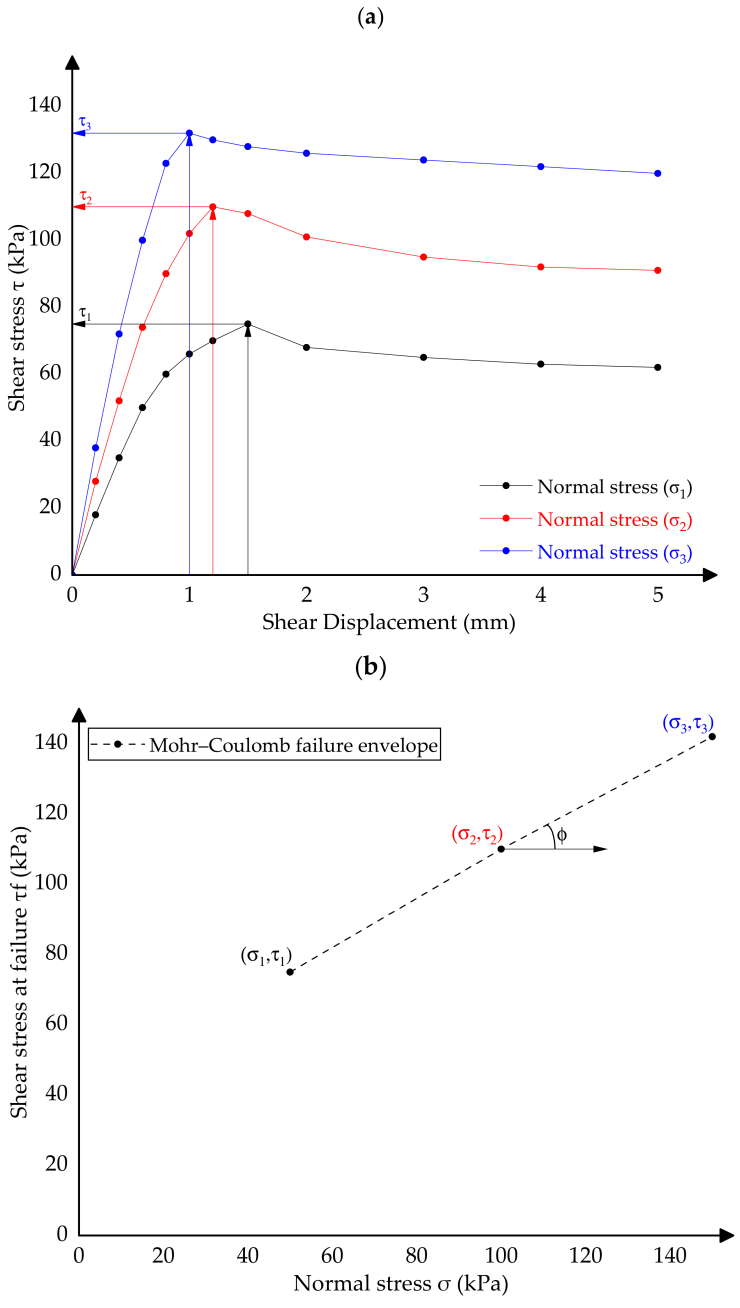


Figure 16. The direct box test results. (**a**) Shear stress–displacement curves under different normal stresses. (**b**) Mohr–Coulomb failure envelope: shear stress at failure vs. normal stress.

The direct box shear test is not typically applied directly to pure SS due to its paste-like rheology and high compressibility but is extensively used when DSS serves as a component in engineered mixtures and construction materials [97,179–181]. These applications leverage the test's ability to quantify Mohr–Coulomb parameters essential for the geotechnical performance of SS-based products.

8.4. Vane Shear Test

The vane shear test is a standardized geotechnical method used to determine the undrained shear strength of cohesive materials under undrained conditions. The method consists of inserting a four-bladed vane into the material and rotating it about its vertical axis at a controlled rate, thereby inducing torsional shear failure along a cylindrical surface surrounding the vane [182]. The test assumes that failure occurs uniformly along this cylindrical surface and that the material behaves as a purely cohesive medium under undrained conditions.

The apparatus typically comprises a four-bladed steel vane attached to a calibrated torque-measuring device. The vane is inserted into the specimen or in situ soil mass to a specified depth, and torque is applied until peak resistance is reached. The undrained shear strength (s_u) is calculated from the maximum measured torque (T_m) using the following relationship for a standard vane geometry:

$$s_u = \frac{T_m}{\pi D^2 \frac{H}{2} + \pi \frac{D^3}{6}}$$

where D is the vane diameter and H corresponds to the vane height. This formulation accounts for shear mobilized along both the cylindrical surface and the top and bottom end surfaces. The vane shear test can be performed both in situ and in the laboratory, and it is widely adopted due to its simplicity, rapid execution, and cost-effectiveness. Figure 17 presents a schematic representation of the vane shear apparatus.

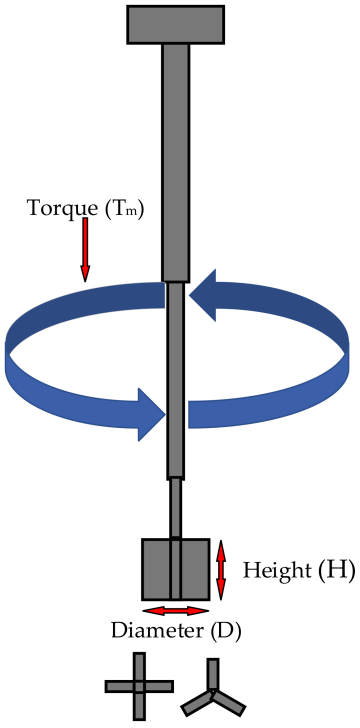


Figure 17. Vane shear test apparatus.

In the context of DSS and faecal sludge, the vane shear test has been extensively applied to determine undrained shear strength for assessing landfill disposal suitability [183], monitoring dewatering efficiency in centrifuge, belt press, and filter press systems, and evaluating chemical conditioning effects [184]. Beyond static strength determination, the test has also been used to investigate thixotropy, yield stress evolution, and material sensitivity in faecal sludge, particularly for pit emptying operations (e.g., VIP latrines), estimation of pipeline restart pressures, and assessment of storage stability, often complemented by field validation using pocket shear metres [169,185]. Additional studies have confirmed its relevance for biosolids geotechnical assessment, thermal drying transitions, and composite material strength characterization [98].

The principal advantage of the vane shear test lies in its ability to measure undrained shear strength without significant sample disturbance and without requiring complex confinement systems. However, its interpretation assumes uniform shear along the failure surface and purely cohesive behaviour, conditions that may not strictly apply to heterogeneous, fibrous, or partially structured sludge systems. Furthermore, rate dependence and structural breakdown during rotation may influence the measured strength, particularly in highly thixotropic DSS. Consequently, while highly suitable for rapid undrained strength estimation, vane shear results should be interpreted with consideration of material structure and testing rate.

8.5. Triaxial Shear Test

The triaxial shear test is a standardized geotechnical method widely used to determine the shear strength parameters of cohesive and semi-solid materials under controlled confinement [186]. The stress conditions imposed on a DSS sample during a triaxial compression test are illustrated in Figure 18. A confining pressure (σ_c) is applied by pressurizing the fluid (generally water) surrounding the sample within the triaxial cell.

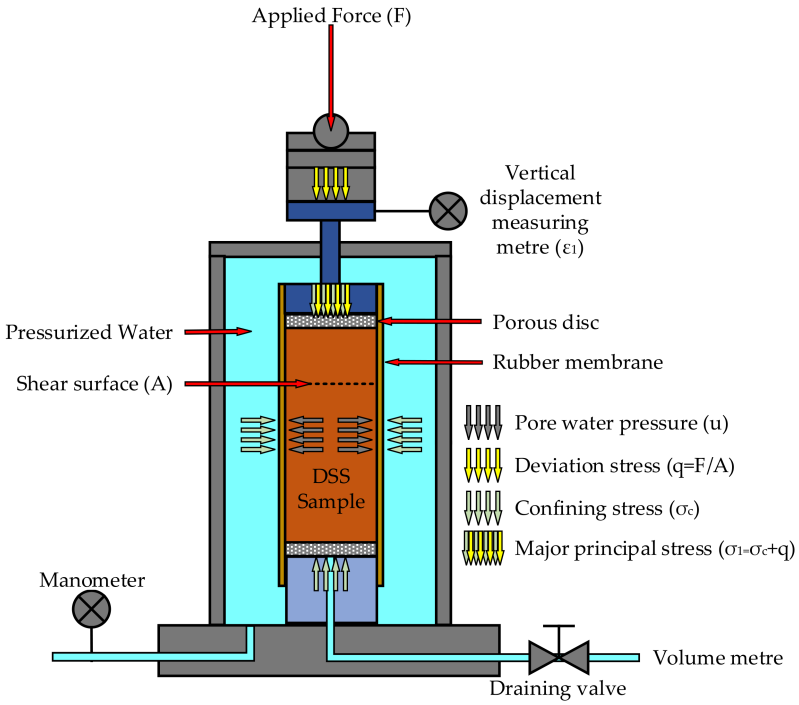


Figure 18. The triaxial apparatus.

An additional stress component, known as the deviator stress (q), is generated by applying an axial deformation (ε_1) to the DSS sample. This loading increases the stress in the vertical direction, producing the axial stress (σ_1), which represents the major principal

stress. The axial stress therefore results from the combination of the confining pressure and the applied deviator stress. A schematic representation of the apparatus is shown in Figure 18.

Depending on drainage conditions, the test may be conducted as consolidated drained (CD), consolidated undrained (CU), or unconsolidated undrained (UU). The resulting stress paths allow the derivation of shear strength parameters, cohesion (c) and internal friction angle (ϕ), through Mohr–Coulomb failure envelopes obtained from tests performed at multiple confining pressures, typically expressed as:

$$\tau_f = c + \sigma' \tan(\phi)$$

where τ_f is the shear stress at failure and σ' is the effective normal stress. Figure 19 shows an example of the obtained results in the triaxial test.

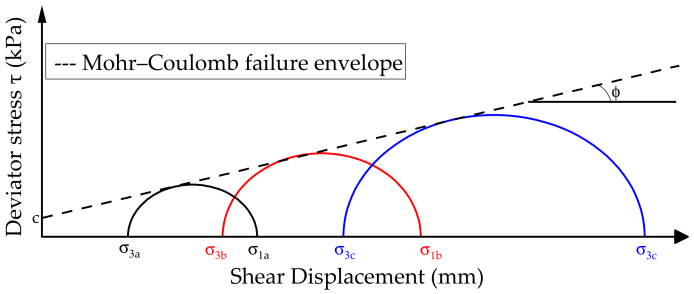


Figure 19. The triaxial test results.

In sludge-related research, the consolidated undrained (CU) configuration is most frequently adopted to simulate landfill burial and confined storage conditions. In sludge-containing municipal solid waste, triaxial testing has revealed a strain-hardening response, characterized by a progressive increase in deviator stress with axial strain rather than a distinct peak failure [181]. Variations in sludge content significantly influence shear strength parameters, primarily through modifications of the internal friction angle under confinement [35,36].

Similarly, in soil stabilization studies, triaxial testing has been employed to evaluate the evolution of shear strength in sludge-derived mixtures prepared under controlled compaction conditions [187]. These studies demonstrate that the method is effective for identifying strength enhancement mechanisms associated with cementitious bonding, as well as strength reductions when excessive sludge-derived material acts predominantly as a void-filling phase.

Although the triaxial test provides robust and reproducible measurements of confined shear behaviour and allows rigorous stress-path control, its application to highly deformable DSS remains challenging. Specimen preparation, membrane installation, and consolidation require sufficient structural integrity, which may not be achievable in highly plastic or weakly structured sludge. Moreover, large volumetric strains and pore pressure redistribution may complicate interpretation. Consequently, while particularly relevant for landfill stability assessment and stabilized sludge systems, the direct applicability of the triaxial test to fresh, highly plastic DSS is more limited compared with rheometric or texture-based techniques.

8.6. Unconfined Compression Test

The unconfined shear test, commonly referred to as the unconfined compression test (UCS), is a standardized method used to determine the undrained shear strength of cohesive materials under zero lateral confinement. In this test, a cylindrical specimen is

subjected to axial compression at a constant strain rate while no confining pressure is applied. The apparatus consists of a vertical loading frame equipped with rigid compression platens, a load cell for force measurement, and a displacement-controlled mechanism to impose constant axial strain, as shown in Figure 20. Standardized specimen geometries are adopted to ensure uniform stress distribution and minimize end-restraint effects. In sludge-related applications, specimens are typically prepared at controlled water content and dry density and may be saturated or subjected to soaking treatments to simulate landfill exposure conditions.

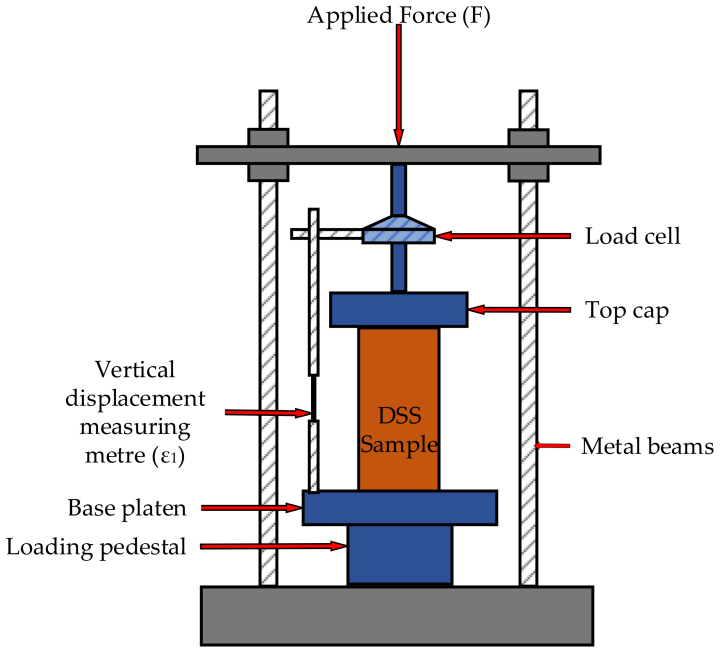


Figure 20. The unconfined compression test apparatus.

An example of unconfined test results is shown in Figure 21, in this graph, the peak axial compressive stress (σ_1) is recorded, and the shear strength (S_u) is commonly estimated as

$$S_u = \frac{\sigma_1}{2}$$

assuming purely cohesive behaviour under undrained conditions.

The application of unconfined shear testing to SS has been widely reported in studies addressing landfill stability and mechanical characterization [36,188–191]. Previous investigations have shown that the undrained shear strength of sludge strongly depends on solid content, establishing a clear relationship between moisture reduction and mechanical resistance [96]. Similarly, DSS has been reported to exhibit measurable undrained strength comparable to soft cohesive soils when sufficient dewatering is achieved [36]. Mechanical testing under axial loading has further demonstrated that sludge behaviour may transition from ductile to brittle depending on organic content, structural conditioning, and degree of consolidation [192].

The application of unconfined shear testing to SS has been reported in the literature in order to characterize its geotechnical characteristics when is mixed with different materials [96,190,191,193]. Overall, the unconfined shear test provides a simple, rapid, and reproducible method for evaluating the intrinsic cohesion and structural integrity of DSS. Its experimental simplicity makes it particularly suitable for comparative studies assessing strength evolution during dewatering, stabilization, or drying processes. However, the absence of lateral confinement limits direct extrapolation to in situ conditions involving

overburden stresses, and highly plastic sludge may undergo significant deformation before reaching peak stress. Despite these limitations, the method remains a reference technique for quantifying undrained shear behaviour in sludge-based materials.

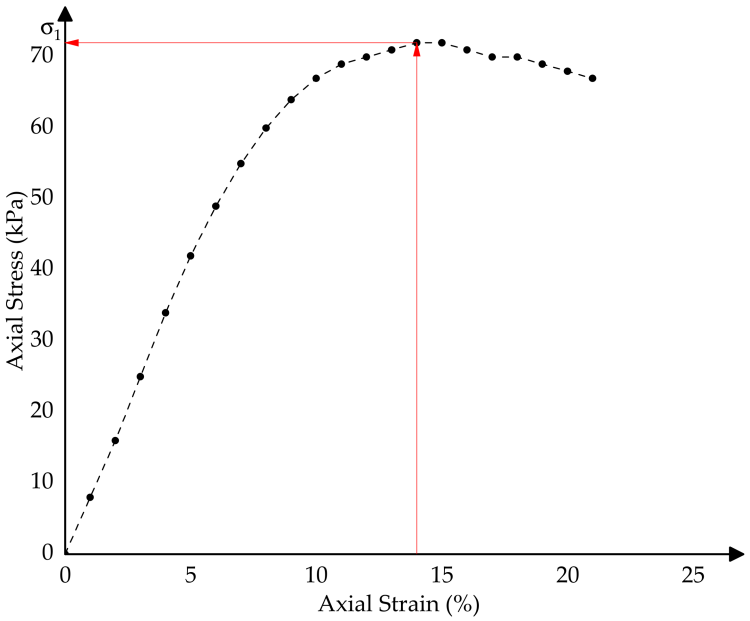


Figure 21. The unconfined test results.

8.7. Jenike Shear Test

The Jenike shear test was developed by Andrew W. Jenike in the 1960s to characterize the flow properties of bulk solids for hopper and silo design. Originally introduced in the framework of powder mechanics, the method is based on the determination of shear strength under controlled normal stress conditions using a shear cell apparatus. In this test, a consolidated sample is subjected to a predefined normal load and subsequently sheared along a horizontal plane while maintaining constant normal stress [17].

Although shear testing had previously been described for evaluating powder stickiness during drying, its systematic application to DSS was first introduced by Peeters in his doctoral work [17]. In this study, the Jenike-type shear protocol was adapted to activated sludge and, for the first time, applied across the entire range of solids content encountered during mechanical dewatering and thermal drying. This approach enabled a continuous mapping of sludge consistency evolution, from fluid-like behaviour to the plastic–rubbery "sticky phase" and finally to a granular dry state, thereby providing a quantitative framework to identify the critical dryness interval associated with maximum stickiness. This contribution represented the first extension of classical powder mechanics concepts to sludge drying processes, establishing shear-based stickiness mapping as a reference methodology for analyzing consistency transitions in DSS.

The Jenike shear concept was later modified to enable independent measurement of sludge-to-wall adhesion and internal sludge cohesion during drying adhesion and cohesion characterization [21]. In this adapted configuration, sludge was placed inside a cylindrical shear cell resting on a heated stainless-steel plate and subjected to a controlled vertical consolidation load. After partial drying to a target moisture content, a horizontal force was progressively applied until sliding occurred. In the adhesion mode, shear failure developed at the sludge–steel interface, whereas in the cohesion mode a circular ring created a defined internal shear plane within the sludge cake. The shear stress was calculated from the critical sliding load normalized by the contact area. A schematic of the modified apparatus is presented in Figure 22.

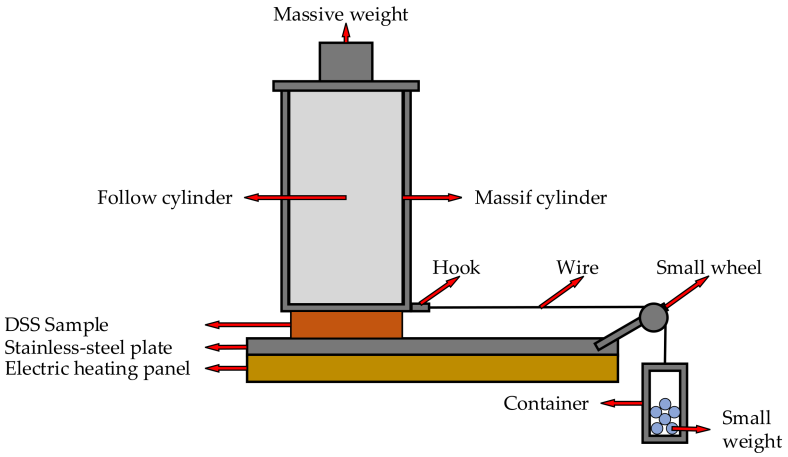


Figure 22. The Jenike test apparatus for DSS.

The shear stress developed at failure was calculated from the critical horizontal force required to initiate sliding. After correction for the blank friction of the apparatus, the shear stress τ was determined as:

$$\tau = \frac{(m - m_0)g}{A}$$

where m is the total applied mass required to induce sliding (kg), m_0 is the blank mass corresponding to the friction of the empty device (kg), g is the gravitational acceleration, and A is the shear contact area (m^2).

In the adhesion configuration, A corresponds to the contact surface between sludge and stainless steel. In the cohesion configuration, A represents the internal shear plane defined by the cylindrical ring.

By repeating the test at different moisture contents, the evolution of shear stress as a function of dryness can be mapped, allowing identification of the maximum shear resistance associated with the sticky phase.

8.8. Compression Tests: Uniaxial Compression and TPA

Compression testing constitutes a robust method for characterizing the mechanical behaviour of highly concentrated and deformable materials such as DSS, for which conventional shear rheometry may be limited by wall slip or premature fracture. In this test, a cylindrical specimen is subjected to controlled axial deformation between two parallel rigid plates while force and displacement are continuously recorded. From these measurements, stress–strain curves can be derived, enabling the identification of elastic deformation, yielding, plastic flow, fracture, and energy dissipation mechanisms. In Figure 23 the compression test is schematized.

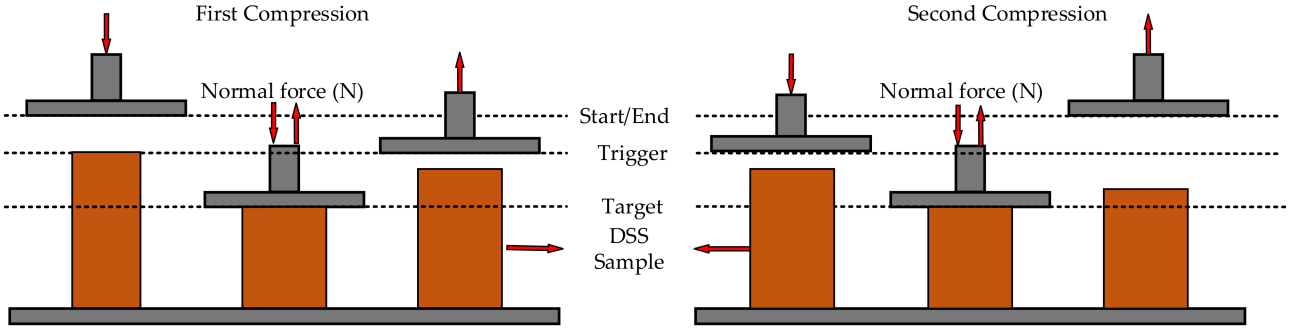


Figure 23. Compression test schematics.

The uniaxial compression test may be performed as a single loading–unloading cycle or repeated over multiple cycles depending on the objective of the analysis. Engineering stress is calculated as $\sigma = \frac{F}{A_0}$, where F is the measured force and A_0 the initial cross-sectional area of the specimen, while engineering strain is defined as $\varepsilon = \frac{\Delta L}{L_0}$ the initial height. For large deformations, true stress–strain formulations may be adopted to account for geometric changes during compression. The area enclosed by the loading–unloading curve represents mechanical energy dissipation associated with viscous effects and internal structural rearrangements, which are particularly relevant in sludge systems.

When conducted as a two-cycle test, the protocol corresponds to the classical Texture Profile Analysis (TPA) [194,195], originally developed in food engineering to quantify empirical textural parameters such as hardness, cohesiveness, adhesiveness, resilience, and springiness. Hardness is defined as the maximum force reached during the first compression; cohesiveness corresponds to the ratio of the work performed during the second compression to that of the first; and adhesiveness is obtained from the negative work measured during probe withdrawal. Although initially applied to food materials, this approach has proven suitable for describing the structural state and handling properties of DSS, particularly during the sticky phase [24,39].

In contrast, the uniaxial rheological framework formalized by Liang interprets the same compression signal within a constitutive modelling perspective [26]. The loading–unloading response is analyzed using visco-elasto-plastic analogue models combining elastic springs, viscous dashpots, and plastic elements, enabling the identification of elastic modulus, yield-like thresholds, viscous coefficients, and strain-hardening parameters. Unlike TPA, which provides phenomenological descriptors, this approach allows quantitative rheological parameter extraction and modelling of sludge behaviour under compressive loading.

A general representation of the force–time response obtained during a double-compression test is shown in Figure 24. The first and second loading cycles are clearly distinguished, separated by a short recovery period. The maximum force reached during the first compression (F_{Max}) defines the hardness, which reflects the resistance of the material to deformation. The negative force recorded during probe withdrawal after the first compression corresponds to adhesiveness, quantified as the absolute value of the negative area under the curve of first compression, representing the mechanical work required to detach the plunger from the sample surface.

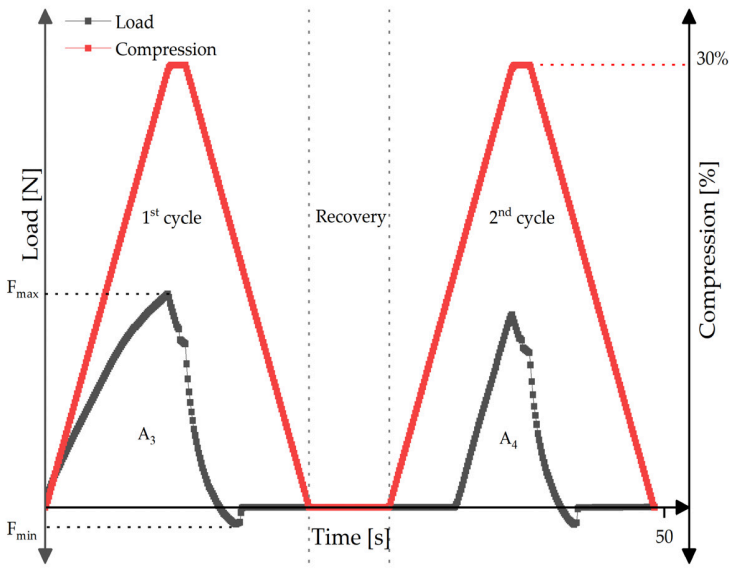


Figure 24. General results obtained from TPA tests.

The positive areas under the force–displacement curves of the first and second compressions (A_1 and A_2 in Figure 24) are used to calculate cohesiveness, defined as the ratio $\frac{A_2}{A_1}$. This dimensionless parameter reflects the ability of the material to withstand a second deformation relative to its initial structural integrity. A value close to unity indicates limited structural damage during the first compression, whereas lower values reveal structural breakdown [194,196,197].

Although additional parameters such as gumminess, springiness, resilience, chewiness, and fracturability can also be derived from the diagram, these descriptors are primarily rooted in food science applications and are less commonly employed in sludge rheological characterization [24,39,195].

Overall, compression testing provides a versatile framework for characterizing the mechanical behaviour of DSS across a wide range of solid contents. When interpreted through the TPA methodology, the test delivers simple and robust empirical descriptors, such as hardness, cohesiveness, and adhesiveness, which are particularly useful for assessing handling properties, stickiness, and structural integrity during drying and mechanical dewatering. These parameters are well suited for identifying critical transitions such as the sticky phase, where surface interactions and structural collapse govern process limitations.

In contrast, the uniaxial rheological modelling approach enables a more mechanistic interpretation of the same experimental signal. By fitting the load–unload response to visco-elasto-plastic constitutive models, quantitative parameters such as elastic modulus, yield-like stress, viscous contributions, and hardening coefficients can be extracted. This framework is especially valuable for simulating sludge behaviour under compressive stresses encountered during storage, extrusion, transport, or landfill confinement.

Therefore, while TPA offers a practical and rapid tool for operational assessment of DSS consistency and stickiness, the uniaxial rheological approach provides deeper insight into the material's constitutive behaviour.

8.9. Controlled Penetration Test (Sphere and Cone)

Controlled penetration tests are mechanical indentation methods used to evaluate the resistance of soft materials to localized deformation. In this approach, a rigid probe is driven into the material while the applied force and the penetration depth are recorded. The resulting force–displacement response provides information on the material's resistance to deformation and reflects the combined effects of compression, shear, and flow within the structure. Because the deformation is localized around the probe, penetration tests are particularly suitable for characterizing soft solids, pastes, and gel-like materials whose mechanical behaviour cannot be easily assessed using conventional bulk mechanical tests [198,199], In Figure 25 the compression test is schematized.

The mechanical response measured during penetration strongly depends on the geometry of the indenter used. Probes with well-defined shapes, most commonly spherical or conical, are employed to ensure reproducible stress distributions during indentation. The contact area between the probe and the material evolves as penetration proceeds, influencing the magnitude of the measured force and the deformation mechanisms activated within the material. Consequently, the probe geometry and dimensions play a critical role in penetration measurements and must be carefully selected when comparing results between different materials or experimental conditions.

In sludge characterization, penetration tests are commonly performed using spherical probes, allowing the extraction of several mechanical indicators from the force–penetration curve. The maximum penetration force (F_{max}) is generally associated with the firmness or resistance of the material to deformation, while the initial slope of the curve provides an indication of the material stiffness during the early stages of indentation. Additional

parameters, such as the work of penetration or the force evolution with depth, can also be derived to describe the consistency and structural resistance of the sludge. An example of the typical force–penetration response obtained from such measurements is presented in Figure 26 [24,49,195,200,201].

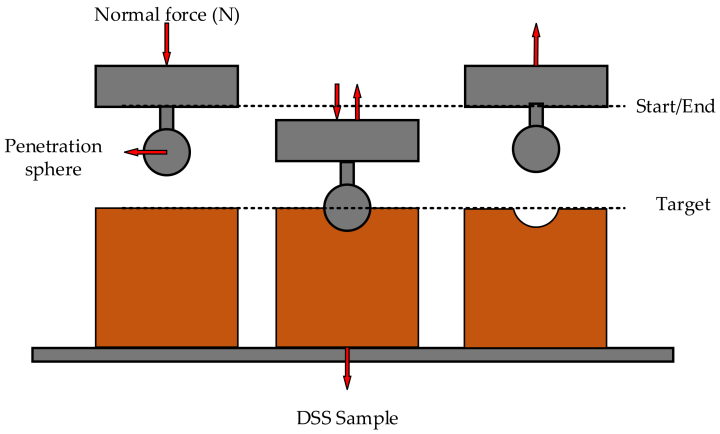


Figure 25. Penetration test schematics.

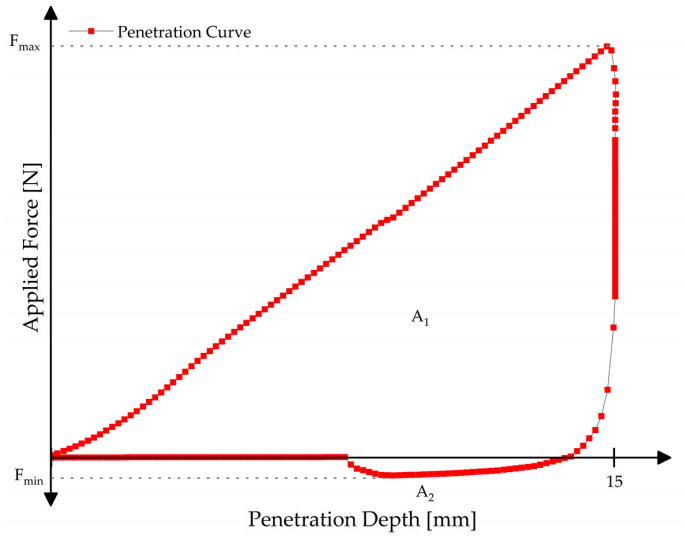


Figure 26. General results obtained from compression tests.

Compared with bulk rheological measurements, penetration tests provide a simple and rapid way to assess the mechanical consistency of sludge using relatively small sample volumes and minimal preparation. The method is particularly suitable for highly heterogeneous or partially structured materials where conventional rheometry may be difficult to apply. However, because the deformation is localized around the indenter, the measured response reflects local resistance rather than the bulk mechanical behaviour of the material. Consequently, penetration measurements are often considered complementary to rheological or compression-based tests, which provide a more global description of the material structure and deformation behaviour.

8.10. Oscillatory Rheometry

Oscillatory rheometry is an advanced characterization technique used to investigate the viscoelastic behaviour of complex materials. The test is performed using a controlled rheometer, in which a small oscillatory deformation (strain-controlled mode) or stress (stress-controlled mode) is applied to the sample while the resulting stress or deformation response is measured. Unlike steady shear tests, oscillatory measurements impose

sinusoidal deformations that allow the simultaneous evaluation of the elastic and viscous contributions to the mechanical response of the material [92,109,202,203]. This method is particularly suitable for structured suspensions such as DSS, where both solid-like and liquid-like behaviours coexist depending on the applied deformation conditions. In Figure 27 the compression test is schematized.

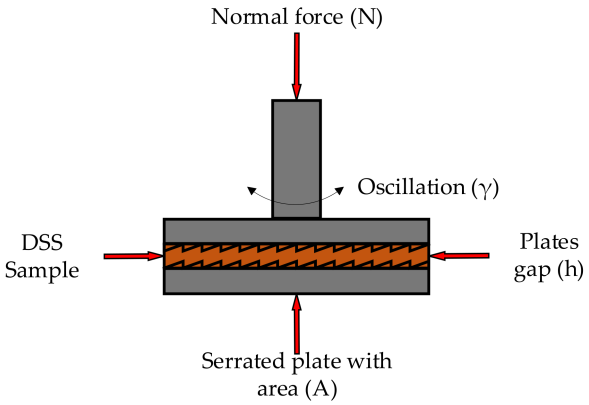


Figure 27. Oscillatory rheology tests schematics.

In oscillatory tests, the viscoelastic response of the material is commonly described using the complex shear modulus (G^*), which is decomposed into two components: the storage modulus (G') and the loss modulus (G''). The storage modulus represents the elastic contribution of the material, reflecting the energy stored during deformation and associated with solid-like behaviour, whereas the loss modulus represents the viscous contribution, corresponding to the energy dissipated as flow. The ratio between these two parameters, often expressed as the loss tangent ($\tan \delta = G''/G'$), provides an indicator of the dominant mechanical response of the material. When G' is higher than G'' the material exhibits predominantly elastic behaviour, while the opposite situation indicates a more viscous or liquid-like response. In concentrated sludge systems, oscillatory rheometry typically reveals a viscoelastic behaviour in which both contributions coexist due to the complex network formed by microorganisms, organic matter, and inorganic particles within the sludge matrix [23,24,38,39,86,195,204,205].

Several oscillatory tests can be performed to characterize the viscoelastic properties of sludge. A strain sweep test is typically conducted first to determine the linear viscoelastic region (LVE), where the structure of the material remains intact and the viscoelastic moduli are independent of the applied deformation. Within this region, the measured rheological parameters reflect the intrinsic structure of the material. Once the LVE is identified, a frequency sweep test can be carried out by varying the oscillation frequency while keeping the deformation constant. This test provides insight into the structural organization and relaxation dynamics of the material, as well as the dominance of elastic or viscous contributions across different time scales. In addition, creep–recovery tests may be performed to evaluate the time-dependent viscoelastic response under a constant applied stress, followed by a recovery phase after stress removal. These complementary tests are commonly used to describe the semi-solid rheological behaviour of sludge and to support the development of viscoelastic models describing its mechanical response [23,24,38,39,86,195,204,205]. An example of the typical rheogram response obtained from such measurements is presented in Figure 28.

In DSS systems, oscillatory rheometry has revealed a strong dependence of viscoelastic behaviour on TSCs and the physicochemical structure of the sludge matrix [39,86]. At low solids concentrations, sludge tends to behave predominantly as a viscous fluid, with G'' exceeding G'. However, as the solids content increases, particularly after thickening or

mechanical dewatering, the structure becomes progressively more interconnected due to stronger particle–particle interactions and the formation of a three-dimensional network of flocs and organic matter. Under these conditions, G' typically becomes higher than G'', indicating a transition toward solid-like viscoelastic behaviour. This structural evolution strongly influences sludge handling and processing operations, including pumping, mixing, dewatering, and drying, making oscillatory rheometry a valuable tool for understanding and predicting sludge behaviour in wastewater treatment processes.

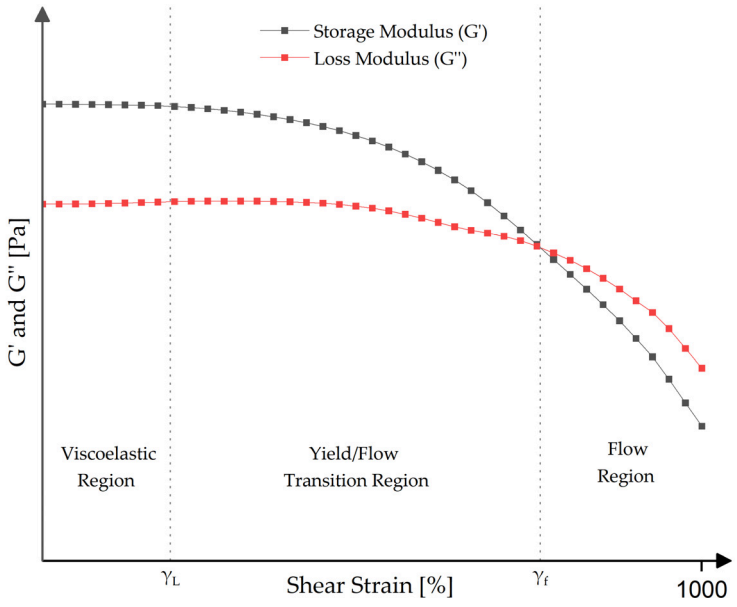


Figure 28. Oscillatory rheology tests general results.

Oscillatory rheometry is one of the most advanced and specialized techniques used for the mechanical characterization of sludge. Its main strength lies in its ability to quantify the viscoelastic properties of the material in a non-destructive manner, allowing detailed investigation of the internal structure, relaxation mechanisms, and structural evolution of sludge under small deformations. This makes the method particularly valuable for developing rheological models and for understanding the behaviour of concentrated or semi-solid sludge during processes such as mixing, dewatering, and drying. However, compared with simpler mechanical tests such as penetration or compression, oscillatory rheometry presents several limitations. The technique requires dedicated rheological instrumentation, careful control of experimental conditions (geometry, temperature, evaporation, and sample preparation), and well-trained personnel to ensure reliable measurements and proper interpretation of the results. In addition, sludge samples are often heterogeneous and sensitive to structural disturbances during loading, which may affect the repeatability of the measurements. Consequently, while oscillatory rheometry provides the most detailed rheological information among the methods discussed, its application is generally limited to laboratory environments and specialized research studies.

9. Comparative Summary of Experimental Methods for Sludge Mechanical Characterization

To facilitate the comparison of the experimental techniques discussed in this section, Table 5 summarizes the main methods used to characterize the mechanical behaviour of sludge, together with the corresponding properties that can be obtained. The table highlights the type of mechanical response probed by each method and indicates whether rheological, viscoelastic, textural, geotechnical, cohesive, or adhesive properties can be determined.

Table 5. Comparison of experimental techniques used to characterize rheological, textural, viscoelastic, and geotechnical properties of soft materials.

Family	Method	Application DS Interval	Main Property Measured	Type of Deformation	Adhesion	Cohesion	Typical Parameters Obtained	Relationship to Other Methods
Compression/textural	Penetration test (sphere/cone)	10–70% [39]	Mechanical consistency	Local indentation	Yes	Yes	F_{max}, penetration work, adhesion force	Within the compression/textural family, penetration, TPA, and uniaxial compression were grouped together because all three impose controlled deformation on DSS and therefore probe how the material resists indentation or compression. The penetration test is particularly suited to assessing mechanical consistency through local indentation and is more directly related to TPA and UCS through the imposed deformation than through the exact stress field. TPA is the closest to uniaxial compression because both tests are based on controlled loading, but TPA is interpreted mainly in terms of textural descriptors such as hardness, cohesiveness, and adhesiveness, whereas uniaxial compression is more often treated as a strength-oriented test that provides a stress–strain response and elastic modulus. For this reason, these methods should be considered complementary approaches within the compression/textural domain rather than direct substitutes.
	Texture Profile Analysis (TPA)	15–45% [39]	Textural properties	Cyclic compression	Yes	Yes	Hardness, cohesiveness, adhesiveness	
	Uniaxial compression test	15–45% [20]	Mechanical strength/texture	Compression	Yes	Yes	Stress–strain curve, elastic modulus, adhesion force	
Geotechnical	Direct shear test	20–45% [181,206]	Shear strength parameters	Shear	No	Yes	Cohesion (c), friction angle (φ)	Within the geotechnical family, direct shear, Jenike shear, triaxial shear, and vane shear were classified as shear strength tests, whereas UCS was classified as a compressive-strength test. Although all of them characterize DSS mechanical resistance, they differ in stress path, confinement, and failure mode, and should therefore be regarded as complementary rather than interchangeable methods. Vane shear is particularly suitable for very wet, cohesive DSS because it mobilizes undrained resistance through rotational loading; triaxial compression provides a more complete strength description by controlling confinement and stress path; direct box shear isolates frictional resistance along a predefined failure plane; and the Jenike shear test is especially useful for mapping the sticky phase and identifying the onset of cohesion-related handling problems. Therefore, these methods should be viewed as complementary approaches to sludge strength characterization rather than direct substitutes.
	Jenike shear test	7–90% [18]	Bulk cohesion/adhesion	Shear	Yes (modified apparatus)	Yes	Cohesive strength, adhesion stress	
	Triaxial shear test	25–70% [35]	Geotechnical strength	Confined compression/shear	No	Yes	c, φ, stress path	
	Unconfined compression test (UCS)	No fixed TS interval	Unconfined compressive strength, cohesion, stress–strain response	Compression	No	No	c, φ, stress path	
	Vane shear test	10–70% [18]	Undrained shear strength	Shear	No	Yes	Undrained shear strength	

Table 5. *Cont.*

Family	Method	Application DS Interval	Main Property Measured	Type of Deformation	Adhesion	Cohesion	Typical Parameters Obtained	Relationship to Other Methods
Rheological	Oscillatory rheometry	15–45% [23,39]	Viscoelastic properties	Small oscillatory deformation	No	Yes (structural)	G', G'', tan δ, LVE	Within the rheological family, oscillatory rheometry and the slump test were grouped together because both aim to capture the deformation behaviour of DSS under conditions that are relevant to flow and structural breakdown, although they do so at very different scales. Oscillatory rheometry is the most fundamental of the two, since it probes viscoelastic properties under small-amplitude oscillatory deformation and yields parameters. In contrast, the slump test is a simpler and lower-cost approach that captures flowability and yield behaviour through gravity-driven deformation, providing practical descriptors such as slump height and apparent yield stress. Therefore, these methods are complementary rather than interchangeable: oscillatory rheometry provides a detailed viscoelastic characterization, whereas the slump test offers a rapid operational estimate of flow-related behaviour.
	Slump test	15–40% [207]	Flowability/yield behaviour	Gravity deformation	No	Yes	Slump height, apparent yield stress	
State classification	Atterberg limits	No fixed TS interval	Visual transitions and Mechanical consistency	Flow	No	No	Liquid limit (*LL*), plastic limit (*PL*), shrinkage limit	Not directly comparable to strength tests; used to classify consistency.

Methods were grouped by response domain rather than treated as interchangeable tests, because compression-based, shear-based, rheological, and state-classification methods probe different mechanical aspects of DSS; comparability is therefore meaningful only within a shared family and solids window.

Figure 29 summarizes the main experimental approaches used to characterize the mechanical behaviour of dewatered sewage sludge and highlights how each method captures a different mechanical domain. The comparison map groups the techniques into four complementary families: compression/textural methods, geotechnical shear strength methods, rheological methods, and state-classification methods. It also shows the typical solids-content ranges where each method is most often applied, illustrating the overlap between methods and the gradual transition from soft cohesive material behaviour to shear-dominated and consistency-based characterization. This overview is intended to guide the reader through the logic of the review and to facilitate the selection of the most appropriate method depending on the property of interest.

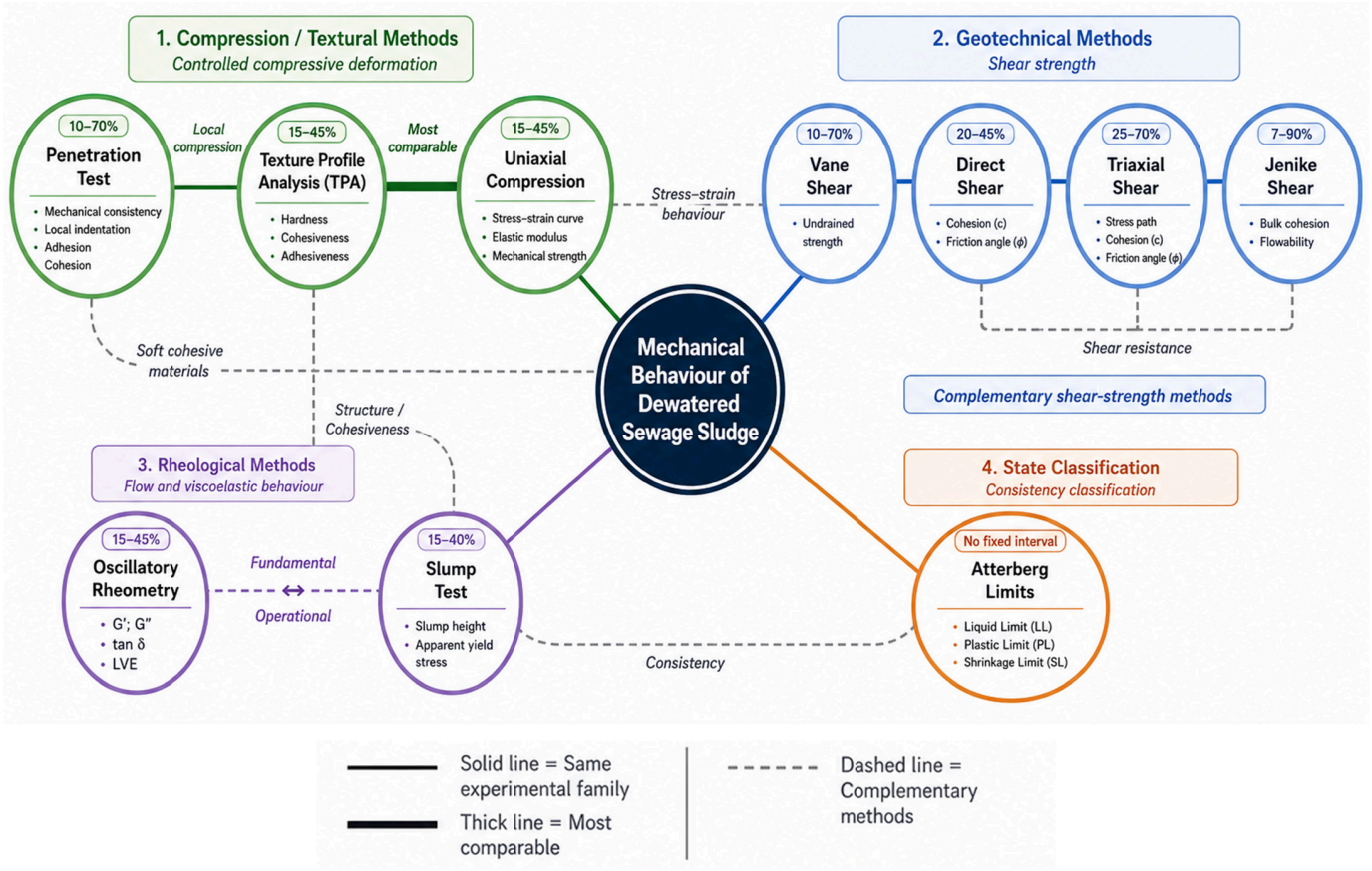


Figure 29. Mechanical characterization map of DSS.

10. Adhesion: An Overlooked Property in Sludge Mechanical Characterization

Despite the wide variety of experimental techniques used to characterize the mechanical behaviour of DSS, most studies have traditionally focused on rheological and geotechnical parameters such yield stress, shear strength, or viscoelastic behaviour. In contrast, adhesion has received comparatively little attention, even though it plays a central role in many practical problems associated with sludge handling as mentioned before.

This imbalance in the literature partly originates from the historical development of sludge characterization methods. Many commonly used tests, such as rheometry, shear tests, or geotechnical strength measurements, were originally designed to quantify bulk me-

chanical properties such as cohesion or flow resistance, rather than interfacial interactions between the sludge and external surfaces. As a result, adhesion has often been considered indirectly or described qualitatively as "stickiness", without being systematically quantified as a mechanical property.

However, as highlighted in Table 5, several experimental methods commonly used for sludge characterization, such as texture profile analysis, uniaxial compression tests, penetration tests, and modified shear tests, can provide direct or indirect measurements of adhesive behaviour when the detachment force or the work required to separate a probe from the material is quantified. These approaches offer promising opportunities to better understand the mechanisms governing sludge stickiness during processes such as dewatering, drying, and storage.

Consequently, future research on sludge mechanics would benefit from a more systematic integration of adhesion measurements into experimental characterization protocols. By combining adhesion measurements with rheological, textural, and geotechnical analyses, a more comprehensive description of sludge mechanical behaviour could be achieved, ultimately improving the design and optimization of sludge treatment and handling processes.

Supplementary Materials: The following supporting information can be downloaded at: https://www.mdpi.com/article/10.3390/adhesives2030015/s1, Table S1. Synonyms used for keyword disambiguation; Table S2. Supplementary File Info Papers.

Author Contributions: Conceptualization, S.L.P.-A. and A.L.; data curation, S.L.P.-A., G.H.G. and J.F.H.-R.; formal analysis, S.L.P.-A., G.H.G. and J.F.H.-R.; investigation, S.L.P.-A., G.H.G. and J.F.H.-R.; methodology, S.L.P.-A., J.F.H.-R. and A.L.; software, S.L.P.-A., G.H.G. and J.F.H.-R.; supervision, A.L.; visualization, S.L.P.-A. and A.L.; writing—original draft S.L.P.-A., A.L., G.H.G. and J.F.H.-R.; writing—review and editing, S.L.P.-A., A.L., G.H.G. and J.F.H.-R.; project administration, A.L.; funding acquisition, A.L. All authors have read and agreed to the published version of the manuscript.

Funding: This work was supported by the Fund for Scientific Research (F.R.S.–FNRS) [T.0159.20-PDR], "Sludge dewatering and drying vs. rheology".

Institutional Review Board Statement: Not applicable.

Informed Consent Statement: Not applicable.

Data Availability Statement: Data are contained within the article.

Acknowledgments: J.F.H.R would like to thank the help and guidance from the Unit of Analysis an Bibliometrics at the Universidad Nacional de Colombia sede Manizales.

Conflicts of Interest: The authors declare no conflicts of interest.

Abbreviations

The following abbreviations are used in this manuscript:

DSS	Dewatered Sewage Sludge
TPA	Texture Profile Analysis
SS	Sewage Sludge
WWTPs	Wastewater Treatment Plants
DSs	Dry Solids
SCs	Scientific Contributions
EPSs	Extracellular Polymeric Substances
CFD	Computational Fluid Dynamics
TB-EPSs	Tightly Bound Extracellular Polymeric Substances
S-EPSs	Soluble Extracellular Polymeric Substances
TSCs	Total Solid Contents
LL	Liquid Limit

PL	Plastic Limit
SL	Shrinking Limit
S	Slump Height
Su	Undrained Shear Strength
φ	Internal Friction Angle
c	Cohesion
η	Viscosity,
τ	Shear Stress
$\dot{\gamma}$	Shear Rate
σ_o	Yield Stress
G^*	Complex Shear Modulus
G'	Storage Modulus
G''	Loss Modulus
LVR	Linear Viscoelastic Region
FL	Flow Point
$\tan(\delta)$	Loss Tangent
σ	Applied Stress
ε	Proportional Deformation
E	Elastic Modulus
Es	Spring
σ_c	Critical Yield Stress
ηd	Dashpot
PI	Plasticity Index
σ_n	Normal Effective Stress
T_m	Maximum Measured Torque
σ_c	Confining Pressure
q	Deviator Stress
CU	Consolidated Undrained Sludge
UCS	Unconfined Compression Test
F_{Max}	Maximum Force reached during the first compression of TPA

References

1. Jiang, Y.; Gao, F.; Zhang, N.; Li, J.; Xu, M.; Jiang, Y. Dehydration Performance of Municipal Sludge and Its Dewatering Conditioning Methods: A Review. *Ind. Eng. Chem. Res.* **2023**, *62*, 11337–11357. [CrossRef]
2. Gao, N.; Kamran, K.; Quan, C.; Williams, P.T. Thermochemical Conversion of Sewage Sludge: A Critical Review. *Prog. Energy Combust. Sci.* **2020**, *79*, 100843. [CrossRef]
3. Eurostat. *Sewage Sludge Production and Disposal*; European Statistical Office: Luxembourg, 2022.
4. Waseem, M.; Khan, M.U.; Bokhary, A.; Ahring, B.K. Emerging Trends in Sewage Sludge Pretreatment: Enhancing Treatment Efficiency and Sustainable Waste Management. *Clean. Water* **2025**, *3*, 100080. [CrossRef]
5. Ben Hamed, H.; Debuigne, A.; Kleinjan, H.; Toye, D.; Léonard, A. Enhancing Sewage Sludge Stabilization, Pathogen Removal, and Biomass Production through Indigenous Microalgae Promoting Growth: A Sustainable Approach for Sewage Sludge Treatment. *Recycling* **2024**, *9*, 97. [CrossRef]
6. Seiple, T.E.; Coleman, A.M.; Skaggs, R.L. Municipal Wastewater Sludge as a Sustainable Bioresource in the United States. *J. Environ. Manag.* **2017**, *197*, 673–680. [CrossRef] [PubMed]
7. Liu, Y.; Zhou, J.; Lu, S.; Ren, J. Towards the New Era of Sewage Sludge Management in China: Status, Challenges, and Perspectives. *Process Saf. Environ. Prot.* **2025**, *198*, 107201. [CrossRef]
8. Nguyen, T.H.; Fujiwara, T.; Yamashita, H.; Togawa, H.; Miyake, H.; Goto, M.; Nagare, H.; Nakamura, M.; Oritate, F.; Ihara, H.; et al. From Sewage Sludge to Agriculture: Governmental Initiatives, Technologies, and Sustainable Practices in Japan. *J. Mater. Cycles Waste Manag.* **2025**, *27*, 2832–2849. [CrossRef]
9. Sude, G.; Rajpal, A.; Tyagi, V.K.; Sharma, K.; Mutiyar, P.K.; Panday, B.K.; Pandey, R.P.; Kazmi, A.A. Evaluation of Sludge Quality in Indian Sewage Treatment Plants to Develop Quality Control Indices. *Environ. Sci. Pollut. Res.* **2023**, *31*, 17578–17590. [CrossRef] [PubMed]
10. Đurđević, D.; Žiković, S.; Blecich, P. Sustainable Sewage Sludge Management Technologies Selection Based on Techno-Economic-Environmental Criteria: Case Study of Croatia. *Energies* **2022**, *15*, 3941. [CrossRef]

11. Ferrentino, R.; Langone, M.; Fiori, L.; Andreottola, G. Full-Scale Sewage Sludge Reduction Technologies: A Review with a Focus on Energy Consumption. *Water* **2023**, *15*, 615. [CrossRef]
12. Chang, H.; Zhao, Y.; Xu, A.; Damgaard, A.; Christensen, T.H. Mini-Review of Inventory Data for the Dewatering and Drying of Sewage Sludge. *Waste Manag. Res. J. A Sustain. Circ. Econ.* **2023**, *41*, 1081–1088. [CrossRef] [PubMed]
13. Mayer, F.; Bhandari, R.; Gäth, S.A. Life Cycle Assessment of Prospective Sewage Sludge Treatment Paths in Germany. *J. Environ. Manag.* **2021**, *290*, 112557. [CrossRef] [PubMed]
14. Eshtiaghi, N.; Markis, F.; Yap, S.D.; Baudez, J.-C.; Slatter, P. Rheological Characterisation of Municipal Sludge: A Review. *Water Res.* **2013**, *47*, 5493–5510. [CrossRef] [PubMed]
15. Infusino, E.; Caloiero, T. Municipal Wastewater Sludge Rheology: Impact of Temperature, Solid Content, and Settling Solids. *Water Environ. Res.* **2021**, *93*, 2971–2981. [CrossRef] [PubMed]
16. Feng, G.; Hu, Z.; Ma, H.; Bai, T.; Guo, Y.; Hao, Y. Semi-Solid Rheology Characterization of Sludge Conditioned with Inorganic Coagulants. *Water Sci. Technol.* **2019**, *80*, 2158–2168. [CrossRef] [PubMed]
17. Peeters, B. Effect of Activated Sludge Composition on Its Dewaterability and Sticky Phase. Ph.D. Thesis, Katholieke Universiteit Leuven, Leuven, Belgium, 2011.
18. Peeters, B.; Dewil, R.; Van Impe, J.F.; Vernimmen, L.; Smets, I.Y. Using a Shear Test-Based Lab Protocol to Map the Sticky Phase of Activated Sludge. *Environ. Eng. Sci.* **2011**, *28*, 81–85. [CrossRef]
19. Yen, P.-S.; Chen, L.C.; Chien, C.Y.; Wu, R.-M.; Lee, D.J. Network Strength and Dewaterability of Flocculated Activated Sludge. *Water Res.* **2002**, *36*, 539–550. [CrossRef] [PubMed]
20. Liang, F.; Sauceau, M.; Dusserre, G.; Arlabosse, P. A Uniaxial Cyclic Compression Method for Characterizing the Rheological and Textural Behaviors of Mechanically Dewatered Sewage Sludge. *Water Res.* **2017**, *113*, 171–180. [CrossRef] [PubMed]
21. Li, B.; Wang, F.; Chi, Y.; Yan, J.H. Adhesion and Cohesion Characteristics of Sewage Sludge During Drying. *Dry. Technol.* **2014**, *32*, 1598–1607. [CrossRef]
22. Mouzaoui, M.; Sauceau, M.; Devriendt, L.; Baudez, J.C.; Arlabosse, P. Rheological Characterization of Sludge in Divided Granular-like and Pasty States Using a Granular Rheometer. *Powder Technol.* **2021**, *378*, 521–527. [CrossRef]
23. Mouzaoui, M.; Baudez, J.C.; Sauceau, M.; Arlabosse, P. Experimental Rheological Procedure Adapted to Pasty Dewatered Sludge up to 45% Dry Matter. *Water Res.* **2018**, *133*, 1–7. [CrossRef] [PubMed]
24. Parra-Angarita, S.L.; Al Sayed, M.W.; Léonard, A. The Variability of Textural Properties and Drying Characteristics of Dehydrated Sewage Sludge. *Clean Technol.* **2025**, *7*, 31. [CrossRef]
25. Wu, B.; Dai, X.; Chai, X. Critical Review on Dewatering of Sewage Sludge: Influential Mechanism, Conditioning Technologies and Implications to Sludge Re-Utilizations. *Water Res.* **2020**, *180*, 115912. [CrossRef] [PubMed]
26. Liang, F.; Sauceau, M.; Dusserre, G.; Dirion, J.-L.; Arlabosse, P. Modelling of the Rheological Behavior of Mechanically Dewatered Sewage Sludge in Uniaxial Cyclic Compression. *Water Res.* **2018**, *147*, 413–421. [CrossRef] [PubMed]
27. Liang, F. Caractérisation et Modélisation Du Comportement Rhéologique Des Boues Résiduaires Urbaines Concentrées. Doctoral Dissertation, Université de Toulouse, Toulouse, France, 2016.
28. Collivignarelli, M.C.; Carnevale Miino, M.; Bellazzi, S.; Caccamo, F.M.; Durante, A.; Abbà, A. Review of Rheological Behaviour of Sewage Sludge and Its Importance in the Management of Wastewater Treatment Plants. *Water Pract. Technol.* **2022**, *17*, 483–491. [CrossRef]
29. Ratkovich, N.; Horn, W.; Helmus, F.P.; Rosenberger, S.; Naessens, W.; Nopens, I.; Bentzen, T.R. Activated Sludge Rheology: A Critical Review on Data Collection and Modelling. *Water Res.* **2013**, *47*, 463–482. [CrossRef] [PubMed]
30. Seyssiecq, I.; Ferrasse, J.-H.; Roche, N. State-of-the-Art: Rheological Characterisation of Wastewater Treatment Sludge. *Biochem. Eng. J.* **2003**, *16*, 41–56. [CrossRef]
31. Baudez, J.-C.; Coussot, P. Rheology of Aging, Concentrated, Polymeric Suspensions: Application to Pasty Sewage Sludges. *J. Rheol.* **2001**, *45*, 1123–1139. [CrossRef]
32. Peeters, B.; Dewil, R.; Smets, I.Y. Challenges of Drying Sticky Wastewater Sludge. *Chem. Eng.* **2014**, *121*, 51–54.
33. Charlou, C. Caractérisation et Modélisation de L'écoulement de Boues Résiduaires Dans Un Sécheur à Palettes. Doctoral Dissertation, Université de Toulouse, Toulouse, France, 2014.
34. O'Kelly, B.C. Fall-Cone Strength Testing of Municipal Sludges and Residues. *Environ. Geotech.* **2018**, *5*, 18–30. [CrossRef]
35. O'Kelly, B.C. Mechanical Properties of Dewatered Sewage Sludge. *Waste Manag.* **2005**, *25*, 47–52. [CrossRef] [PubMed]
36. O'Kelly, B.C. Geotechnical Properties of Municipal Sewage Sludge. *Geotech. Geol. Eng.* **2006**, *24*, 833–850. [CrossRef]
37. Krishnan, J.; Juneja, A.; Solanki, C.H. Determination of Shear Strength, Shear Viscosity and Liquidity Index Using Fall Cone Penetrometer. In *Proceedings of the Indian Geotechnical Conference 2019*; Springer: Singapore, 2021; pp. 33–45.
38. Huron, Y.; Salmon, T.; Crine, M.; Blandin, G.; Léonard, A. Effect of Liming on the Convective Drying of Urban Residual Sludges. *Asia-Pac. J. Chem. Eng.* **2010**, *5*, 909–914. [CrossRef]
39. Parra-Angarita, S.L.; Essanoussi, M.; Ben Hamed, H.; Fantasse, A.; Léonard, A. Dewatered Sewage Sludge Textural and Viscoelastic Changes during Its Drying: Focus on the Sticky Phase. *Desalin. Water Treat.* **2025**, *324*, 101576. [CrossRef]

40. Hong, E.; Yeneneh, A.M.; Sen, T.K.; Ang, H.M.; Kayaalp, A. A Comprehensive Review on Rheological Studies of Sludge from Various Sections of Municipal Wastewater Treatment Plants for Enhancement of Process Performance. *Adv. Colloid Interface Sci.* **2018**, *257*, 19–30. [CrossRef] [PubMed]
41. Liu, G.-J.; Deng, L.-W. Rheological Properties of Anaerobic Sludge. *Environ. Technol. Rev.* **2017**, *6*, 199–208. [CrossRef]
42. Sava, C.; Iluţiu-Varvara, D.-A.; Mare, R.; Roman, M.D.; Rada, S.; Pică, E.M.; Jäntschi, L. Physico-Chemical Characterization and Possible Uses of Sludge Processed from an Urban Sewage Treatment Plant. *Heliyon* **2024**, *10*, e29576. [CrossRef] [PubMed]
43. Terekhin, A.P.; Maryandyshev, P.A.; Brillard, A. Investigation of the Morphology, Composition, and Structure of Dehydrated Sewage Sludge of a Pulp and Paper Enterprise. *Solid Fuel Chem.* **2024**, *58*, 459–464. [CrossRef]
44. Zhang, S.; Du, Q.; Cheng, K.; Antonietti, M.; Yang, F. Efficient Phosphorus Recycling and Heavy Metal Removal from Wastewater Sludge by a Novel Hydrothermal Humification-Technique. *Chem. Eng. J.* **2020**, *394*, 124832. [CrossRef]
45. Sommers, L.E. Chemical Composition of Sewage Sludges and Analysis of Their Potential Use as Fertilizers. *J. Environ. Qual.* **1977**, *6*, 225–232. [CrossRef]
46. Sommers, L.E.; Nelson, D.W.; Yost, K.J. Variable Nature of Chemical Composition of Sewage Sludges. *J. Environ. Qual.* **1976**, *5*, 303–306. [CrossRef]
47. Hurynovich, A.; Kwietniewski, M.; Romanovski, V. Evaluation of the Possibility of Utilization of Sewage Sludge from a Wastewater Treatment Plant—Case Study. *Desalin. Water Treat.* **2021**, *227*, 16–25. [CrossRef]
48. Rodrigues, M.M.; Viana, D.G.; Mendonça, R.S.; Capra, G.F.; Oliveira, F.C.; da Silva, L.F.V.; Nogueira, T.A.R.; Regitano, J.B. Critical Analysis of Sewage Sludge-Based Organomineral Fertilizers through a Bibliometric Perspective. *Environ. Dev. Sustain.* **2025**. [CrossRef]
49. Al, H.; Judenne, E.; Remy, M. The Effect of Lime Treatment on Sludge Rheological Properties. In Proceedings of the 10th European Biosolids and Biowaste Conference, Wakefield, UK, 13–16 November 2005.
50. Kopp, J.; Dichtl, N. Influence of the Free Water Content on the Dewaterability of Sewage Sludges. *Water Sci. Technol.* **2001**, *44*, 177–183. [CrossRef]
51. Kopp, J.; Dichtl, N. Prediction of Full-Scale Dewatering Results by Determining the Water Distribution of Sewage Sludges. *Water Sci. Technol.* **2000**, *42*, 141–149. [CrossRef]
52. Vaxelaire, J.; Cézac, P. Moisture Distribution in Activated Sludges: A Review. *Water Res.* **2004**, *38*, 2215–2230. [CrossRef] [PubMed]
53. Möller, U.K. Water Binding. In *Sludge Characteristics and Behavior*; Springer: Dordrecht, The Netherlands, 1983; pp. 182–194.
54. Rayavellore Suryakumar, A.K.; Mercer, E.; Pocock, J.; Septien, S. Determination of Unbound-Bound Moisture Interface of Faecal Sludges from Different on-Site Sanitation Systems. *Heliyon* **2025**, *11*, e42091. [CrossRef] [PubMed]
55. To, V.H.P.; Nguyen, T.V.; Vigneswaran, S.; Ngo, H.H. A Review on Sludge Dewatering Indices. *Water Sci. Technol.* **2016**, *74*, 1–16. [CrossRef] [PubMed]
56. Huang, L.; Jin, Y.; Zhou, D.; Liu, L.; Huang, S.; Zhao, Y.; Chen, Y. A Review of the Role of Extracellular Polymeric Substances (EPS) in Wastewater Treatment Systems. *Int. J. Environ. Res. Public Health* **2022**, *19*, 12191. [CrossRef] [PubMed]
57. Chen, W.; Gao, X.; Xu, H.; Cai, Y.; Cui, J. Influence of Extracellular Polymeric Substances (EPS) Treated by Combined Ultrasound Pretreatment and Chemical Re-Flocculation on Water Treatment Sludge Settling Performance. *Chemosphere* **2017**, *170*, 196–206. [CrossRef] [PubMed]
58. Liu, H.; Fang, H.H.P. Extraction of Extracellular Polymeric Substances (EPS) of Sludges. *J. Biotechnol.* **2002**, *95*, 249–256. [CrossRef] [PubMed]
59. Atmakuri, A.; Yadav, B.; Tiwari, B.; Drogui, P.; Tyagi, R.D.; Wong, J.W.C. Nature's Architects: A Comprehensive Review of Extracellular Polymeric Substances and Their Diverse Applications. *Waste Dispos. Sustain. Energy* **2024**, *6*, 529–551. [CrossRef]
60. Liu, Y.; Fang, H.H.P. Influences of Extracellular Polymeric Substances (EPS) on Flocculation, Settling, and Dewatering of Activated Sludge. *Crit. Rev. Environ. Sci. Technol.* **2003**, *33*, 237–273. [CrossRef]
61. Chen, M.Y.; Lee, D.J.; Tay, J.H. Distribution of Extracellular Polymeric Substances in Aerobic Granules. *Appl. Microbiol. Biotechnol.* **2007**, *73*, 1463–1469. [CrossRef] [PubMed]
62. Yuan, H.; Zhu, N. Progress of Improving Waste Activated Sludge Dewaterability: Influence Factors, Conditioning Technologies and Implications and Perspectives. *Sci. Total Environ.* **2024**, *912*, 168605. [CrossRef] [PubMed]
63. Ruiz, T.; Kaosol, T.; Wisniewski, C. Dewatering of Urban Residual Sludges: Filterability and Hydro-Textural Characteristics of Conditioned Sludge. *Sep. Purif. Technol.* **2010**, *72*, 275–281. [CrossRef]
64. Pambou, Y.B.; Fraikin, L.; Salmon, T.; Crine, M.; Léonard, A. Sludge Dewatering and Drying: About the Difficulty of Making Experiments with a Non-Stabilized Material. *Desalin. Water Treat.* **2016**, *57*, 13841–13856. [CrossRef]
65. Pambou, Y.B.; Fraikin, L.; Salmon, T.; Crine, M.; Léonard, A. Enhanced Sludge Dewatering and Drying Comparison of Two Linear Polyelectrolytes Co-Conditioning with Polyaluminum Chloride. *Desalin. Water Treat.* **2016**, *57*, 27989–28006. [CrossRef]
66. Novak, J.T. Dewatering of Sewage Sludge. *Dry. Technol.* **2006**, *24*, 1257–1262. [CrossRef]
67. Semiyaga, S.; Okure, M.A.E.; Niwagaba, C.B.; Nyenje, P.M.; Kansiime, F. Dewaterability of Faecal Sludge and Its Implications on Faecal Sludge Management in Urban Slums. *Int. J. Environ. Sci. Technol.* **2017**, *14*, 151–164. [CrossRef]

68. Yu, W.; Li, P.S. Determine the Moisture Distribution in Sewage Sludge by Drying Differential. *Appl. Mech. Mater.* **2014**, *665*, 404–407. [CrossRef]
69. Deng, W.; Li, X.; Yan, J.; Wang, F.; Chi, Y.; Cen, K. Moisture Distribution in Sludges Based on Different Testing Methods. *J. Environ. Sci.* **2011**, *23*, 875–880. [CrossRef] [PubMed]
70. Rao, B.; Wang, G.; Xu, P. Recent Advances in Sludge Dewatering and Drying Technology. *Dry. Technol.* **2022**, *40*, 3049–3063. [CrossRef]
71. Deng, W.-Y.; Yuan, M.-H.; Mei, J.; Liu, Y.-J.; Su, Y.-X. Effect of Calcium Oxide (CaO) and Sawdust on Adhesion and Cohesion Characteristics of Sewage Sludge under Agitated and Non-Agitated Drying Conditions. *Water Res.* **2017**, *110*, 150–160. [CrossRef] [PubMed]
72. Kudra, T. Sticky Region in Drying—Definition and Identification. *Dry. Technol.* **2003**, *21*, 1457–1469. [CrossRef]
73. Arlabosse, P.; Chavez, S.; Prevot, C. Drying of Municipal Sewage Sludge: From a Laboratory Scale Batch Indirect Dryer to the Paddle Dryer. *Braz. J. Chem. Eng.* **2005**, *22*, 227–232. [CrossRef]
74. Li, H.; Zou, S.; Li, Y.; Jin, Y. Characteristics and Model of Sludge Adhesion during Thermal Drying. *Environ. Technol.* **2013**, *34*, 807–812. [CrossRef] [PubMed]
75. Deng, W.; Xiao, J.; Lai, Z.; Su, Y. A New Method to Characterize Sludge Stickiness during Drying: Effects of Sludge Temperature and Calcium Oxide (CaO) on Stickiness. *Dry. Technol.* **2020**, *38*, 1107–1120. [CrossRef]
76. Mupinga, R.T.; Mercer, E.; Rayavellore Suryakumar, A.; Pocock, J.; Septien, S. Insight into the Stickiness of Faecal Sludge from Dry Sanitation Technologies: A Path toward Sustainable and Efficient FSM via Thermal Processes. *Results Eng.* **2025**, *26*, 105453. [CrossRef]
77. Mupinga, R.T.; Septien, S.; Pocock, J.; Buckley, C. An Investigation into the Stickiness of Faecal Sludge: Preliminary Investigation of VIP and UDDT Sludge with Varying Moisture Content at Ambient Temperature. *Gates Open Res.* **2020**, *4*, 78.
78. Chen, X.; Huang, X.; Tan, H.; Li, Y.; Cao, H.; Jin, Y.; Li, Y.; Wang, X. Effect of Sand Content on Adhesion and Cohesion of Municipal Sludge during Drying Practices: The Characteristics and Modification. *Dry. Technol.* **2024**, *42*, 2268–2277. [CrossRef]
79. Kiper, J.; Głowacka, A.; Rucińska, T. Analysis of the Variability of the Composition of Sewage Sludge Before and After Drying Treatment—SEM Studies. *J. Ecol. Eng.* **2019**, *20*, 45–52. [CrossRef] [PubMed]
80. Léonard, A.; Blacher, S.; Marchot, P.; Pirard, J.-P.; Crine, M. Image Analysis of X-ray Microtomograms of Soft Materials during Convective Drying: 3D Measurements. *J. Microsc.* **2005**, *218*, 247–252. [CrossRef] [PubMed]
81. Leonard, A.; Blacher, S.; Marchot, P.; Crine, M. Use of X-Ray Microtomography to Follow the Convective Heat Drying of Wastewater Sludges. *Dry. Technol.* **2002**, *20*, 1053–1069. [CrossRef]
82. Léonard, A.; Blacher, S.; Marchot, P.; Pirard, J.P.; Crine, M. Measurement of Shrinkage and Cracks Associated to Convective Drying of Soft Materials by X-Ray Microtomography. *Dry. Technol.* **2004**, *22*, 1695–1708. [CrossRef]
83. Tsotsas, E.; Mujumdar, A.S. *Modern Drying Technology, Experimental Techniques*; John Wiley & Sons: Hoboken, NJ, USA, 2011.
84. Bennamoun, L.; Arlabosse, P.; Léonard, A. Review on Fundamental Aspect of Application of Drying Process to Wastewater Sludge. *Renew. Sustain. Energy Rev.* **2013**, *28*, 29–43. [CrossRef]
85. Chen, G.; Lock Yue, P.; Mujumdar, A.S. Sludge Dewatering and Drying. *Dry. Technol.* **2002**, *20*, 883–916. [CrossRef]
86. Schober, A.; Segovia-Gutiérrez, J.P.; Rapf, M.; Drunsel, F.; Duelli, G.; Germann, N. Pilot Drying-Grinding System for Pulverized Sewage Sludge Production. *Open Transp.* **2026**, *1*, 20260002. [CrossRef]
87. Li, J.; Fraikin, L.; Salmon, T.; Toye, D.; Léonard, A. Influence of Back-Mixing on the Convective Drying of Sewage Sludge: The Structural Characteristics. *Dry. Technol.* **2022**, *40*, 205–212. [CrossRef]
88. Zhang, Q.; Wang, B.; Xing, Y.; Wang, G.; Zhang, X.; Lü, X. Drying Characteristics of Sewage Sludge Pre-Conditioned by CaO and Sawdust under Low-Temperature Drying Conditions. *Environ. Technol.* **2024**, *45*, 6237–6248. [CrossRef] [PubMed]
89. Wang, G.; Zhang, K.; Huang, B.; Zhang, K.; Chao, C. Microwave Drying of Sewage Sludge: Process Performance and Energy Consumption. *Processes* **2024**, *12*, 432. [CrossRef]
90. Barnes, H.A.; Hutton, J.F.; Walters, K. *An Introduction to Rheology*; Elsevier: Amsterdam, The Netherlands, 1989.
91. Malkin, A.Y.; Isayev, A.I. *Rheology*; Elsevier: Amsterdam, The Netherlands, 2022.
92. Miri, T. Viscosity and Oscillatory Rheology. In *Practical Food Rheology*; Wiley: Hoboken, NJ, USA, 2011; pp. 7–28.
93. Mewis, J.; Wagner, N.J. *Colloidal Suspension Rheology*; Knovel: New York, NY, USA, 2021.
94. O'Kelly, B.C. Geotechnical Properties of a Municipal Water Treatment Sludge Incorporating a Coagulant. *Can. Geotech. J.* **2008**, *45*, 715–725. [CrossRef]
95. O'Kelly, B.C. Geotechnical Laboratory Testing and Data Interpretation for Biosolids and Sewage Sludge. *Geotech. Res.* **2018**, *5*, 247–261. [CrossRef]
96. Chen, P.; Zhan, L.; Wilson, W. Experimental Investigation on Shear Strength and Permeability of a Deeply Dewatered Sewage Sludge for Use in Landfill Covers. *Environ. Earth Sci.* **2014**, *71*, 4593–4602. [CrossRef]
97. Syafrudin; Hardyanti, N.; Samadikun, B.P.; Budihardjo, M.A.; Ramadan, B.S.; Puspita, A.S.; Arumdani, I.S.; Wati, H.R. Geostability of Dewatered Sludge as Landfill Cover Material. *Glob. Nest J.* **2022**, *25*, 77–83. [CrossRef]

98. Zhan, T.L.; Zhan, X.; Lin, W.; Luo, X.; Chen, Y. Field and Laboratory Investigation on Geotechnical Properties of Sewage Sludge Disposed in a Pit at Changan Landfill, Chengdu, China. *Eng. Geol.* **2014**, *170*, 24–32. [CrossRef]
99. Fernandez-Nieves, A.; Puertas, A.M. *Fluids, Colloids, and Soft Materials: An Introduction to Soft Matter Physics*; John Wiley & Sons, Inc.: Hoboken, NJ, USA, 2016.
100. Cheng, Y.; Li, H. Rheological Behavior of Sewage Sludge with High Solid Content. *Water Sci. Technol.* **2015**, *71*, 1686–1693. [CrossRef] [PubMed]
101. Malczewska, B.; Biczyński, A. Comparison between Different Models for Rheological Characterization of Sludge from Settling Tank. *J. Water Land Dev.* **2017**, *34*, 191–196. [CrossRef]
102. Markis, F.; Baudez, J.-C.; Parthasarathy, R.; Slatter, P.; Eshtiaghi, N. Rheological Characterisation of Primary and Secondary Sludge: Impact of Solids Concentration. *Chem. Eng. J.* **2014**, *253*, 526–537. [CrossRef]
103. Cao, X.; Jiang, Z.; Cui, W.; Wang, Y.; Yang, P. Rheological Properties of Municipal Sewage Sludge: Dependency on Solid Concentration and Temperature. *Procedia Environ. Sci.* **2016**, *31*, 113–121. [CrossRef]
104. Wei, P. Characterisation of Sludge Rheology and Sludge Mixing in Gas-Mixed Anaerobic Digesters. Doctoral Dissertation, TU Delft, Delft, The Netherlands, 2021.
105. Telis, V.R.N.; Telis-Romero, J.; Gabas, A.L. Solids Rheology for Dehydrated Food and Biological Materials. *Dry. Technol.* **2005**, *23*, 759–780. [CrossRef]
106. Fielding, S.M.; Sollich, P.; Cates, M.E. Aging and Rheology in Soft Materials. *J. Rheol.* **2000**, *44*, 323–369. [CrossRef]
107. Baudez, J.-C.; Gupta, R.K.; Eshtiaghi, N.; Slatter, P. The Viscoelastic Behaviour of Raw and Anaerobic Digested Sludge: Strong Similarities with Soft-Glassy Materials. *Water Res.* **2013**, *47*, 173–180. [CrossRef] [PubMed]
108. Zhang, J.; Haward, S.J.; Wu, Z.; Dai, X.; Tao, W.; Li, Z. Evolution of Rheological Characteristics of High-Solid Municipal Sludge During Anaerobic Digestion. *Appl. Rheol.* **2016**, *26*, 32973. [CrossRef]
109. Mezger, T.G. *The Rheology Handbook: For Users of Rotational and Oscillatory Rheometers*; Vincentz Network: Hannover, Germany, 2006.
110. Creton, C.; Ciccotti, M. Fracture and Adhesion of Soft Materials: A Review. *Rep. Prog. Phys.* **2016**, *79*, 046601. [CrossRef] [PubMed]
111. Gerberich, W.W.; Cordill, M.J. Physics of Adhesion. *Rep. Prog. Phys.* **2006**, *69*, 2157–2203. [CrossRef]
112. Lee, L.H. *Adhesive Bonding*; Springer: Berlin/Heidelberg, Germany, 2013.
113. Rowlinson, J.S. *Cohesion: A Scientific History of Intermolecular Forces*; Cambridge University Press: Cambridge, UK, 2005.
114. Abbott, S. *Adhesion Science: Principles and Practice*; DEStech Publications: Lancaster, PA, USA, 2015.
115. Li, Z.; Li, H.; Zhao, L.; Liu, X.; Wan, C. Understanding the Role of Cations and Hydrogen Bonds on the Stability of Aerobic Granules from the Perspective of the Aggregation and Adhesion Behavior of Extracellular Polymeric Substances. *Sci. Total Environ.* **2021**, *795*, 148659. [CrossRef] [PubMed]
116. Caudan, C.; Filali, A.; Spérandio, M.; Girbal-Neuhauser, E. Multiple EPS Interactions Involved in the Cohesion and Structure of Aerobic Granules. *Chemosphere* **2014**, *117*, 262–270. [CrossRef] [PubMed]
117. Adav, S.S.; Lee, D.-J.; Tay, J.-H. Extracellular Polymeric Substances and Structural Stability of Aerobic Granule. *Water Res.* **2008**, *42*, 1644–1650. [CrossRef] [PubMed]
118. Raynaud, M.; Vaxelaire, J.; Olivier, J.; Dieudé-Fauvel, E.; Baudez, J.-C. Compression Dewatering of Municipal Activated Sludge: Effects of Salt and PH. *Water Res.* **2012**, *46*, 4448–4456. [CrossRef] [PubMed]
119. Wang, L.-F.; Qian, C.; Jiang, J.-K.; Ye, X.-D.; Yu, H.-Q. Response of Extracellular Polymeric Substances to Thermal Treatment in Sludge Dewatering Process. *Environ. Pollut.* **2017**, *231*, 1388–1392. [CrossRef] [PubMed]
120. Yeo, Y.; Jang, N.; Cho, J.; Kim, K.-S.; Kim, I.S. Identification of the Effect of Extracellular Polymeric Substances on Bacterial Adhesion to the Membrane Surface in a Membrane Bioreactor Using Pseudomonas Fluorescens. *Water Sci. Technol.* **2007**, *55*, 35–42. [CrossRef] [PubMed]
121. Li, J.; Hermelijn, J.; van Loosdrecht, M.C.M.; Lin, Y. Adhesion and Binding Properties of Extracellular Polymeric Substances (EPS) Extracted from Activated Sludge. *Bioresour. Technol.* **2026**, *451*, 134544. [CrossRef] [PubMed]
122. Yoo, J.; Oshita, K.; Kusakabe, T.; Takaoka, M. Adhesion Behavior of Dewatered Sewage Sludge during Indirect Thermal Drying. *J. Environ. Manag.* **2025**, *381*, 125203. [CrossRef] [PubMed]
123. Ayol, A.; Dentel, S.K.; Filibeli, A. Toward Efficient Sludge Processing Using Novel Rheological Parameters: Dynamic Rheological Testing. *Water Sci. Technol.* **2006**, *54*, 17–22. [CrossRef] [PubMed]
124. Ju, B.F.; Liu, K.-K. Characterizing Viscoelastic Properties of Thin Elastomeric Membrane. *Mech. Mater.* **2002**, *34*, 485–491. [CrossRef]
125. de Souza Mendes, P.R. Modeling the Thixotropic Behavior of Structured Fluids. *J. Non-Newton. Fluid Mech.* **2009**, *164*, 66–75. [CrossRef]
126. Segalen, C. Complémentarité Des Propriétés Électriques et Rhéologiques Pour Une Caractérisation Des Boues Résiduaires. Doctoral Dissertation, Université Blaise Pascal-Clermont-Ferrand II, Aubière, France, 2014.

127. Quignon-Tosoni, J. Rhéologie Des Matériaux Pâteux: Vers Un Continuum Des Régimes Solide et Liquide: Application Aux Boues Résiduaires. Doctoral Dissertation, Université Blaise Pascal-Clermont-Ferrand II, Aubière, France, 2015.
128. Aria, M.; Cuccurullo, C.; D'Aniello, L.; Misuraca, M.; Spano, M. Comparative Science Mapping: A Novel Conceptual Structure Analysis with Metadata. *Scientometrics* **2024**, *129*, 7055–7081. [CrossRef]
129. Macías-Quiroga, I.F.; Henao-Aguirre, P.A.; Marín-Flórez, A.; Arredondo-López, S.M.; Sanabria-González, N.R. Bibliometric Analysis of Advanced Oxidation Processes (AOPs) in Wastewater Treatment: Global and Ibero-American Research Trends. *Environ. Sci. Pollut. Res.* **2021**, *28*, 23791–23811. [CrossRef] [PubMed]
130. de Oliveira, U.R.; Espindola, L.S.; da Silva, I.R.; da Silva, I.N.; Rocha, H.M. A Systematic Literature Review on Green Supply Chain Management: Research Implications and Future Perspectives. *J. Clean. Prod.* **2018**, *187*, 537–561. [CrossRef]
131. Singh, V.K.; Singh, P.; Karmakar, M.; Leta, J.; Mayr, P. The Journal Coverage of Web of Science, Scopus and Dimensions: A Comparative Analysis. *Scientometrics* **2021**, *126*, 5113–5142. [CrossRef]
132. Zuluaga, M.; Robledo, S.; Arbelaez-Echeverri, O.; Osorio-Zuluaga, G.A.; Duque-Méndez, N. Tree of Science—ToS: A Web-Based Tool for Scientific Literature Recommendation. Search Less, Research More! *Issues Sci. Technol. Librariansh.* **2022**. [CrossRef]
133. Aria, M.; Cuccurullo, C. Bibliometrix: An R-Tool for Comprehensive Science Mapping Analysis. *J. Informetr.* **2017**, *11*, 959–975. [CrossRef]
134. Xia, L.; Hao, X.; Zhou, Y. Machine Learning-Based Global Trends and the Development Prospects of Wastewater Treatment: A Bibliometric Analysis. *J. Environ. Chem. Eng.* **2024**, *12*, 112732. [CrossRef]
135. Perianes-Rodriguez, A.; Waltman, L.; van Eck, N.J. Constructing Bibliometric Networks: A Comparison between Full and Fractional Counting. *J. Informetr.* **2016**, *10*, 1178–1195. [CrossRef]
136. van Eck, N.J.; Waltman, L. Software Survey: VOSviewer, a Computer Program for Bibliometric Mapping. *Scientometrics* **2010**, *84*, 523–538. [CrossRef] [PubMed]
137. Herrera-Ruiz, J.F.; Fontalvo, J.; Prado-Rubio, O.A. Advances on Hybrid Modelling for Bioprocesses Engineering: Insights into Research Trends and Future Directions from a Bibliometric Approach. *Results Eng.* **2024**, *24*, 103548. [CrossRef]
138. Herrera-Ruiz, J.F.; Fontalvo, J.; Prado-Rubio, O.A. Hybrid Modeling for Bioprocesses: Architectures, Applications, and Perspectives. *Eng. Rep.* **2025**, *7*, e70502. [CrossRef]
139. Barriga-Gómez, D.C.; Herrera-Ruiz, J.F.; Morales-Rodriguez, R.; Prado-Rúbio, O.A. Innovative Technologies for Succinic Acid Fermentation: A Path to Sustainable Production. *Chem. Eng. Process. Process Intensif.* **2026**, *221*, 110693. [CrossRef]
140. Ames, W.F.; Behn, V.C. Application of the Method of Composition and Linear Regression Analysis to a Problem Involving a Pseudoplastic Suspension. *Trans. Soc. Rheol.* **1961**, *5*, 53–66. [CrossRef]
141. Kelessidis, A.; Stasinakis, A.S. Comparative Study of the Methods Used for Treatment and Final Disposal of Sewage Sludge in European Countries. *Waste Manag.* **2012**, *32*, 1186–1195. [CrossRef] [PubMed]
142. CEC (Council of the European Communities). *Council Directive of 26 April 1999, on the Land Ll of Waste (99/31/EC)*; European Union: Brussels, Belgium, 1999. Available online: https://eur-lex.europa.eu/eli/dir/1999/31/oj/eng (accessed on 8 April 2026).
143. CEC (Council of the European Communities). *Council Directive of 21 May 1991 Concerning Urban Waste Water Treatment*; European Union: Brussels, Belgium, 1991. Available online: https://eur-lex.europa.eu/eli/dir/1991/271/oj/eng (accessed on 8 April 2026).
144. CEC (Council of the European Communities). *Commission Decision of 16 January 2001 Amending Decision 2000/532/EC as Regards the List of Wastes*; European Union: Brussels, Belgium, 2001. Available online: https://eur-lex.europa.eu/eli/dec/2001/118(1)/oj (accessed on 8 April 2026).
145. Subbanna, M.; Pradip; Malghan, S.G. Shear Yield Stress of Flocculated Alumina–Zirconia Mixed Suspensions. *Chem. Eng. Sci.* **1998**, *53*, 3073–3079. [CrossRef]
146. Chang, I.L.; Lee, D.J. Ternary Expression Stage in Biological Sludge Dewatering. *Water Res.* **1998**, *32*, 905–914. [CrossRef]
147. Jorand, F.; Boué-Bigne, F.; Block, J.C.; Urbain, V. Hydrophobic/Hydrophilic Properties of Activated Sludge Exopolymeric Substances. *Water Sci. Technol.* **1998**, *37*, 307–315. [CrossRef]
148. Dick, R.I.; Ewing, B.B. The Rheology of Activated Sludge. *J. Water Pollut. Control Fed.* **1967**, *39*, 543–560. [PubMed]
149. Donthu, N.; Kumar, S.; Mukherjee, D.; Pandey, N.; Lim, W.M. How to Conduct a Bibliometric Analysis: An Overview and Guidelines. *J. Bus. Res.* **2021**, *133*, 285–296. [CrossRef]
150. Bornmann, L.; Haunschild, R.; Mutz, R. Growth Rates of Modern Science: A Latent Piecewise Growth Curve Approach to Model Publication Numbers from Established and New Literature Databases. *Humanit. Soc. Sci. Commun.* **2021**, *8*, 224. [CrossRef]
151. Aria, M.; Misuraca, M.; Spano, M. Mapping the Evolution of Social Research and Data Science on 30 Years of Social Indicators Research. *Soc. Indic. Res.* **2020**, *149*, 803–831. [CrossRef]
152. Bradford, S.C. CLASSIC PAPER: Sources of Information on Specific Subjects. *Collect. Manag.* **1976**, *1*, 95–104. [CrossRef]
153. Brookes, B.C. Theory of the Bradford Law. *J. Doc.* **1977**, *33*, 180–209. [CrossRef]
154. Krasowska, A.; Sigler, K. How Microorganisms Use Hydrophobicity and What Does This Mean for Human Needs? *Front. Cell. Infect. Microbiol.* **2014**, *4*, 112. [CrossRef] [PubMed]
155. Barber, W.P.F. Thermal Hydrolysis for Sewage Treatment: A Critical Review. *Water Res.* **2016**, *104*, 53–71. [CrossRef] [PubMed]

156. Liu, J.; Wei, Y.; Li, K.; Tong, J.; Wang, Y.; Jia, R. Microwave-Acid Pretreatment: A Potential Process for Enhancing Sludge Dewaterability. *Water Res.* **2016**, *90*, 225–234. [CrossRef] [PubMed]
157. Li, Y.; Zhu, Y.; Wang, D.; Yang, G.; Pan, L.; Wang, Q.; Ni, B.-J.; Li, H.; Yuan, X.; Jiang, L.; et al. Fe(II) Catalyzing Sodium Percarbonate Facilitates the Dewaterability of Waste Activated Sludge: Performance, Mechanism, and Implication. *Water Res.* **2020**, *174*, 115626. [CrossRef] [PubMed]
158. Bougrier, C.; Albasi, C.; Delgenès, J.P.; Carrère, H. Effect of Ultrasonic, Thermal and Ozone Pre-Treatments on Waste Activated Sludge Solubilisation and Anaerobic Biodegradability. *Chem. Eng. Process. Process Intensif.* **2006**, *45*, 711–718. [CrossRef]
159. Su, K.-Z.; Yu, H.-Q. Formation and Characterization of Aerobic Granules in a Sequencing Batch Reactor Treating Soybean-Processing Wastewater. *Environ. Sci. Technol.* **2005**, *39*, 2818–2827. [CrossRef] [PubMed]
160. Kuzma, S.; Bierkens, M.F.P.; Lakshman, S.; Luo, T.; Saccoccia, L.; Sutanudjaja, E.H.; Van Beek, R. *Aqueduct 4.0: Updated Decision-Relevant Global Water Risk Indicators*; World Resources Institute: Washington, DC, USA, 2023. [CrossRef]
161. Kitajima, K.; Okamura, K. The Altering Landscape of US–China Science Collaboration: From Convergence to Divergence. *Humanit. Soc. Sci. Commun.* **2025**, *12*, 302. [CrossRef]
162. Haigh, S.K. Mechanics of the Casagrande Liquid Limit Test. *Can. Geotech. J.* **2012**, *49*, 1015–1023. [CrossRef]
163. Vardanega, P.J.; Haigh, S.K. Some Recent Developments in the Determination of the Atterberg Limits. In *Advances in Transportation Geotechnics and Materials for Sustainable Infrastructure*; American Society of Civil Engineers: Reston, VA, USA, 2014; pp. 48–55.
164. *ASTM D4318-10*; Standard Test Methods for Liquid Limit, Plastic Limit, and Plasticity Index of Soils. ASTM: West Conshohocken, PA, USA, 2018.
165. Standard Methods Committee of the American Public Health Association; American Water Works Association; Water Environment Federation. 2710 TESTS ON SLUDGES. In *Standard Methods For the Examination of Water and Wastewater*; APHA Press: Washington, DC, USA, 2022.
166. *ASTM D3441-16*; ASTM Test Method for Mechanical Cone Penetration Testing of Soils. ASTM: West Conshohocken, PA, USA, 2025.
167. O'Kelly, B.C.; Vardanega, P.J.; Haigh, S.K. Use of Fall Cones to Determine Atterberg Limits: A Review. *Géotechnique* **2018**, *68*, 843–856. [CrossRef]
168. O'Kelly, B.C. Atterberg Limits Are Not Appropriate for Peat Soils. *Geotech. Res.* **2015**, *2*, 123–134. [CrossRef]
169. Shafiq, Y.; Haigh, S.; Holm, R.; Parker, A. Re-Evaluating the Strength of Pit-Latrine Faecal Sludge from Dynamic Cone Penetrometer Test Data. *Water SA* **2020**, *46*, 638–644. [CrossRef]
170. *ASTM C143/C143M-20*; ASTM Test Method for Slump of Hydraulic-Cement Concrete. ASTM: West Conshohocken, PA, USA, 2026.
171. Murata, J. Flow and Deformation of Fresh Concrete. *Matér. Constr.* **1984**, *17*, 117–129. [CrossRef]
172. Baudez, J.-C.; Ayol, A.; Coussot, P. Practical Determination of the Rheological Behavior of Pasty Biosolids. *J. Environ. Manag.* **2004**, *72*, 181–188. [CrossRef] [PubMed]
173. Pashias, N.; Boger, D.V.; Summers, J.; Glenister, D.J. A Fifty Cent Rheometer for Yield Stress Measurement. *J. Rheol.* **1996**, *40*, 1179–1189. [CrossRef]
174. Baudez, J.-C.; Chabot, F.; Coussot, P. Rheological Interpretation of the Slump Test. *Appl. Rheol.* **2002**, *12*, 133–141. [CrossRef]
175. Baudez, J.C. Pourquoi Les Boues Ne Tiennent Pas En Tas. *Environ. Ingénierie Dév.* **2003**, *32*, 3–7.
176. *ASTM D3080/D3080M-23*; Standard Test Method for Direct Shear Test of Soils Under Consolidated Drained Conditions. ASTM International: West Conshohocken, PA, USA, 2023. Available online: https://store.astm.org/d3080_d3080m-23.html (accessed on 8 April 2026).
177. Barla, G.; Barla, M.; Martinotti, M.E. Development of a New Direct Shear Testing Apparatus. *Rock Mech. Rock Eng.* **2010**, *43*, 117–122. [CrossRef]
178. Matsuoka, H.; Liu, S. Simplified Direct Box Shear Test on Granular Materials and Its Application to Rockfill Materials. *Soils Found.* **1998**, *38*, 275–284. [CrossRef] [PubMed]
179. Simoni, A.; Houlsby, G.T. The Direct Shear Strength and Dilatancy of Sand–Gravel Mixtures. *Geotech. Geol. Eng.* **2006**, *24*, 523–549. [CrossRef]
180. Amin Shafii, M.; Mohammad Noh, N. Soft Soil Stabilization Using Sewage Sludge Ash. *ARPN J. Eng. Appl. Sci.* **2018**, *13*, 8280–8284.
181. Zheng, J.; Zhang, Z.; Ke, H.; Lan, J.; Wang, C. Effect of Sludge Content on the Shear Strength Characteristics of Municipal Solid Waste. *Int. J. Environ. Sci. Technol.* **2026**, *23*, 298. [CrossRef]
182. *ASTM D2573-08*; ASTM Test Method for Field Vane Shear Test in Cohesive Soil. ASTM: West Conshohocken, PA, USA, 2008.
183. Blümel, W.; von Bloh, G. Determination of Shear Strength of Different Sludges-Methods and Effects. In *Third International Landflll Symposium*; Sardinlla; Italian Ministry of Environment: Rome, Italy, 1991; pp. 14–18.
184. Koenig, A.; Bari, Q.H. Vane Shear Strength of Dewatered Sludge from Hong Kong. *Water Sci. Technol.* **2001**, *44*, 389–397. [CrossRef]
185. Septien, S.; Pocock, J.; Teba, L.; Velkushanova, K.; Buckley, C.A. Rheological Characteristics of Faecal Sludge from VIP Latrines and Implications on Pit Emptying. *J. Environ. Manag.* **2018**, *228*, 149–157. [CrossRef] [PubMed]

186. *ASTM D4767-11*; ASTM Test Method for Consolidated Undrained Triaxial Compression Test for Cohesive Soils. ASTM: West Conshohocken, PA, USA, 2020.
187. Matthew Ayininuola, G.; Olumuyiwa Ayodeji, I. Influence of Sludge Ash on Soil Shear Strength. *J. Civ. Eng. Res.* **2016**, *6*, 72–77. [CrossRef]
188. Delegard, C.; Schmidt, A.; Chenault, J. *Strength Measurements of Archive K Basin Sludge Using a Soil Penetrometer*; Pacific Northwest National Laboratory (PNNL): Richland, WA, USA, 2011.
189. Baĝrıaçık, B.; Güner, E.D. An Experimental Investigation of Reinforcement Thickness of Improved Clay Soil with Drinking Water Treatment Sludge as an Additive. *KSCE J. Civ. Eng.* **2020**, *24*, 3619–3627. [CrossRef]
190. An, K.; Zhuang, D.; Lin, W.; Argilaga, A.; Chen, Y.; Zhan, L. Field Treatment of Storage Sludge and Stability Analysis of Overlying Municipal Waste Landfilling. *Appl. Sci.* **2021**, *11*, 12102. [CrossRef]
191. Wichmann, K.; Riehl, A. Mechanical Properties of Waterwork Sludges—Shear Strength. *Water Sci. Technol.* **1997**, *36*, 43–50. [CrossRef]
192. Stone, R.J.; Ekwue, E.I.; Clarke, R.O. Engineering Properties of Sewage Sludge in Trinidad. *J. Agric. Eng. Res.* **1998**, *70*, 221–230. [CrossRef]
193. Zhou, A.; Sheng, D. Yield Stress, Volume Change, and Shear Strength Behaviour of Unsaturated Soils: Validation of the SFG Model. *Can. Geotech. J.* **2009**, *46*, 1034–1045. [CrossRef]
194. Nishinari, K.; Kohyama, K.; Kumagai, H.; Funami, T.; Bourne, M.C. Parameters of Texture Profile Analysis. *Food Sci. Technol. Res.* **2013**, *19*, 519–521. [CrossRef]
195. Rayavellore Suryakumar, A.K.; Parra-Angarita, S.L.; Léonard, A.; Pocock, J.; Septien, S. Mechanical Properties of Faecal Sludge and Its Influence on Moisture Retention. *ChemEngineering* **2024**, *9*, 2. [CrossRef]
196. Rosenthal, A.J. Texture Profile Analysis—How Important Are The Parameters? *J. Texture Stud.* **2010**, *41*, 672–684. [CrossRef]
197. Peleg, M. The Instrumental Texture Profile Analysis Revisited. *J. Texture Stud.* **2019**, *50*, 362–368. [CrossRef] [PubMed]
198. Deman, J.M. Food Texture Measurements with The Penetration Method. *J. Texture Stud.* **1969**, *1*, 114–119. [CrossRef] [PubMed]
199. Jonkers, N.; van Dommelen, J.A.W.; Geers, M.G.D. Intrinsic Mechanical Properties of Food in Relation to Texture Parameters. *Mech. Time Depend. Mater.* **2022**, *26*, 323–346. [CrossRef]
200. Pambou, Y.-B. Influence Du Conditionnement et de La Déshydratation Mécanique Sur Le Séchage de Boues d'épuration. Doctoral Thesis, Université de Liège, Liège, Belgium, 2016.
201. Azeddine, F.; Sergio, P.A.; Angélique, L.; El Khadir, L.; Ali, I.; El Houssayne, B. Rheological Behavior and Characterization of Drinking Water Treatment Sludge from Morocco. *Clean Technol.* **2023**, *5*, 259–273. [CrossRef]
202. Tabilo-Munizaga, G.; Barbosa-Cánovas, G.V. Rheology for the Food Industry. *J. Food Eng.* **2005**, *67*, 147–156. [CrossRef]
203. Chen, D.T.N.; Wen, Q.; Janmey, P.A.; Crocker, J.C.; Yodh, A.G. Rheology of Soft Materials. *Annu. Rev. Condens. Matter Phys.* **2010**, *1*, 301–322. [CrossRef]
204. Mouzaoui, M.; Baudez, J.C.; Sauceau, M.; Arlabosse, P. How to Avoid Evaporation during Rheological Measurements of Dewatered Pasty Sludge at High Temperature. *Water Sci. Technol.* **2019**, *79*, 1503–1510. [CrossRef] [PubMed]
205. Santos, A.F.; Ferreira, A.G.M.; Quina, M.J. Efficient Management of Sewage Sludge from Urban Wastewaters with the Addition of Inorganic Waste: Focus on Rheological Properties. *Clean Technol.* **2022**, *4*, 841–853. [CrossRef]
206. Adamczyk, J. Strength and Strain Properties of Coal Sludge. *Appl. Sci.* **2025**, *15*, 12360. [CrossRef]
207. Garcia-Bernet, D.; Loisel, D.; Guizard, G.; Buffière, P.; Steyer, J.P.; Escudié, R. Rapid Measurement of the Yield Stress of Anaerobically-Digested Solid Waste Using Slump Tests. *Waste Manag.* **2011**, *31*, 631–635. [CrossRef] [PubMed]

Disclaimer/Publisher's Note: The statements, opinions and data contained in all publications are solely those of the individual author(s) and contributor(s) and not of MDPI and/or the editor(s). MDPI and/or the editor(s) disclaim responsibility for any injury to people or property resulting from any ideas, methods, instructions or products referred to in the content.